UNIVERSIDAD DE CONCEPCIÓN
FACULTAD DE CIENCIAS FÍSICAS Y MATEMÁTICAS

RESURGENCE IN CRYSTALS OF GAUGED SOLITONS

Por: Gonzalo Enrique Barriga Sanhueza

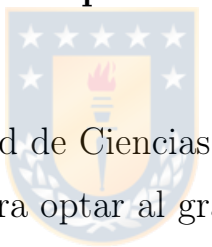

Tesis presentada a la Facultad de Ciencias Físicas y Matemáticas de la Universidad de Concepción para optar al grado académico de Magíster en Ciencias con Mención en Física

Marzo 2021

Concepción, Chile

Director de Tesis : Dr. Fabrizio Canfora Tartaglia

Comisión : Dr. Julio Oliva Zapata

Dr. Fernando Izaurieta Aranda

A mis abuelos...

"Lo esencial de toda exploración será volver al propio jardín y ver las cosas por primera vez."

— T. S. Eliot

AGRADECIMIENTOS

En primer lugar agradecer a mis abuelos y a mis padres por darme todo lo que necesité (y mucho más), sin su amor y apoyo incondicional no habría sido posible este trabajo.

Quiero agradecer enormemente el apoyo y la guia del profesor Fabrizio Canfora quien además de darme un problema en el que trabajar, siempre me ayudo y aconsejo con sinceras palabras. Fue realmente un placer trabajar con él. Agradezco enormemente sus enseñanzas, su paciencia y su amistad.

También quiero agradecer a los profesores que me guiaron durante mi paso por la Universidad de Concepción. Especialmente agradecer al profesor Julio Oliva por su constante apoyo durante mi formación en pregrado y postgrado, su ayuda y sus consejos fueron siempre enriquecedores. Agradecer a los profesores Fernando Izaurieta y Guillermo Rubilar por sus notables clases y siempre responder amablemente todas mis dudas.

Quiero agradecer enormemente a las funcionarias de la Universidad de Concepción Soledad Daroch y Julia Herrera por siempre tener una buena disposición para responder todas mis consultas. Infinitas gracias por su ayuda y consideración.

Agradecer a mis compañeros de trabajo durante esta investigación por su ayuda y su entrega: Matias Torres, Marcela Lagos y Aldo Vera. Fue un placer trabajar con ustedes. Muchas gracias por sus consejos y su compañía.

Por supuesto agradecer a mis amigos y compañeros de generación, aprendí mucho de ellos y estoy seguro que serán grandes investigadores.

Especialmente agradecer a mis amigos de muchos años y compañeros de hogar durante mi paso por Concepción: Jeremy y Daniel, gracias por su amistad y apoyo. Agradecer enormemente a Marta por siempre tener palabras de aliento en los momentos difíciles y por su amor.

Resumen

En esta tesis mostramos que el modelo sigma no lineal acoplado a un campo de gauge $U(1)$ en (3+1) dimensiones posee soluciones analiticas las cuales a respresentan solitones a densidad Barionica finita. Estos solitones generan su propio campo electromagnético el cual satisface la condición de un plasma libre de fuerza (FFP). Luego mostramos que las perturbaciones del perfil de los solitones están relacionadas con operadores del tipo Lamé lo que permite usar la teoría de resurgencia en el estudio de ciertos fonones del sistema. Por otro lado, también realizamos perturbaciones electromagnéticas, estas perturbaciones satisfacen una ecuaciones tipo Schrödinger efectiva donde el fondo de solitones interactúa con las perturbaciones electromagnéticas a través de un potencial periodico en dos dimensiones espaciales. Estudiamos numéricamente el espectro de bandas de energía para diferentes parámetros de la teoría y encontramos que las bandas de energía están moduladas por la intensidad del potencial.Finalmente comparamos nuestras soluciones de cristal con las del modelo de Gross-Neveu en (1+1) dimensiones.

Keywords – Resurgence, Solitons, QCD, FFP

Abstract

We show that the (3+1)-dimensional gauged non-linear sigma model minimally coupled to a $U(1)$ gauge field possesses analytic solutions representing gauged solitons at finite Baryon density whose electromagnetic field is a Force Free Plasma. These gauged solitons present a crystaline structure at finite density and generate in a very natural way persistent currents able to support Force Free Plasma electromagnetic fields. Quite surprisingly, despite the non-integrable nature of the theory, some of the perturbations of these gauged solitons allows to identify a proper resurgent parameter. In particular, the perturbations of the solitons profile are related to the Lamé operator with a suitable “resurgent parameter". On the other hand, the electromagnetic perturbations of the above system satisfy a two dimensional effective Schrödinger equation, where the soliton's background interacts with the electromagnetic pertubations trought an effective two-dimensional periodic potential. We study numerically the band energy spectrum for different values of the free parameters of the theory and we found that bands-gaps are moduleted by the potential strength. Finally we compare our crystal solutions with those of the (1+1)-dimesional Gross-Neveu model.

Keywords – Resurgence, Solitons, QCD, FFP

Contents

AGRADECIMIENTOS i

Resumen ii

Abstract iii

1 Introduction 1

2 Resurgence theory basics 5
2.1 Basic Ingredients of Resurgence theory . . . 6
2.1.1 Borel Transform . . . 6
2.1.2 Borel resummation and Stokes rays . . . 8
2.1.3 Trans-series . . . 9
2.2 Canonical Example: Airy Equation . . . 10
2.2.1 Integral representation of the Airy function . . . 13
2.3 Resurgence in Physics . . . 15

3 Crystal structures in the (3+1)-D gauged non-linear sigma model 17
3.1 The action of the gauged Non-Linear Sigma model . . . 18
3.2 Gauged crystals . . . 19
3.2.1 Te ansatz . . . 19
3.2.2 Field equations . . . 20
3.2.3 Topological charge and energy density . . . 22
3.3 Force Free Plasma Condition . . . 24
3.3.1 Emergent force free plasma . . . 25
3.3.2 Trajectory of charged particles on the FFP . . . 26

4 Resurgence in the fluctuations of the fields 30
4.1 Pertubative analysis . . . 30
4.1.1 Perturbations on the U field . . . 31
4.1.2 Electromagnetic perturbations . . . 34
4.2 Resurgence Structures in the fluctuations . . . 36
4.2.1 WKB Analysis for the SU(2) perturbations . . . 37
4.2.2 Numerical Results . . . 40

4.3 A comparison with the (1+1)-dimensional crystals in the Gross-Neveu model 40

5 Conclusions **44**

References **45**

Appendix **53**

A1 Obtaining the field equations 53

List of Figures

2.1.1 Borel ζ-plane. The zone of convergence delimited by the circumference 7
2.1.2 Contour deformation in the calculation of the discontinuity. 9
2.2.1 Plot of the Airy function $\mathrm{Ai}(z)$ as a function of z. We put in blue the oscillatory behaviour for $z < 0$ and in red exponentially suppress behaviour for $z > 0$ 10
2.2.2 Borel ζ-plane. The zone of convergence delimited by the blue circumference and the logarithmic singularity at $\zeta = -4/3$ 12
2.2.3 Steepest descent contours for $\mathrm{Ai}(z)$ in complex t plane. There are two saddles for any z, given by $t^2 + z = 0$. Blue (black) dots show locations of saddles for negative (positive) z. For $z < 0$, both saddles contribute through contours C_1 and C_2. For $z > 0$, only one saddle contributes, via contour C_3. 14

3.2.1 Comparison of the energy density for different configurations with topological charge $B = 5$, as function of q and m. Here we have considered $n = 5$, $K = 2$, $L = 1$ and $p = 1$. 24
3.3.1 Electric field, magnetic field and the current of two gauged solitons, with $n = 2$, $m = 0$, and $p = q = 1$. The electric and magnetic fields vanish in the center of the tubes while the current is completely contained inside these. 27
3.3.2 Electric field lines and magnetic field lines of two gauged solitons, with $n = 2, m = 0$, and $p = q = 1$. 28
3.3.3 Trayectory of a single particle under the Lorentz force in a time interval between 0 and 1 in (a), a time interval between 1 and 50 in (b) and a time interval between 490 and 500 in (c). The arrow denotes the "increasing time direction" on the trajectory of the test particle. The dots on the trajectory have been taken at equal time interval. Thus, regions where neighbouring dots are "far apart" correspond to "high velocity" regions of the trajectory. 29

4.2.1 Energy Spectrum for Lamé operators from $SU(2)$ perturbations for $m = 0.2$ in (a) and $m = 0.7$ in (b). The regions of stability (the bands) are shaded and they are separated by regions of instability (gaps), which are unshaded. We see a similar behaviour to the Mathieu spectrum in wich at small g, the bands are exponentially narrow and high in the spectrum, the gaps are exponentially narrow. 39
4.2.2 The complex Borel plane for elliptic modulus $m = 0.9$, dots indicating poles of the Borel-Padé approximation obtained from 100 orders of perturbation theory in g^2 (hence we computed a total of 50 poles). Accumulations of poles are anticipated to encode branch cuts in the full Borel transform, and isolated poles are expected to be residuals of the numerical approximation. 39
4.2.3 r-component of two dimensional potential for the perturbed Maxwell equations: $\sin^2(\alpha(r))$ with $n = 1$ and $n = 10$ 41
4.2.4 the Energy Spectrum for the potential $L^2 \sin(\alpha(r))^2 \sin(\theta)^2$ as a function of L, where $\alpha(r)$ is a numerical solution of Eq. (4.2.7) with $n = 1$ 41

Chapter 1

Introduction

The current paradigm for studying physical quantities of practical interest in a Quantum Field Theory and Quantum Mechanics is by perturbation theory. This paradigm has turned out to be very useful to match both theoretical and experimental data. To give just one example, in order to extract relevant physical information from the new LHC data (see [16]) it is necessary to compare the results of the experiment with precise theoretical predictions arising from the radiative corrections in the Standard Model. This requires to go to five-loops computations and beyond. The modern techniques to compute higher loops radiative corrections are quite well equipped for these kinds of tasks. One can already find in the literature of more than ten years ago quite non-trivial higher loops computations (see [29] and references therein). The theoretical techniques needed to assist experiments such as the LHC are in a very good shape and, above all, they can be developed in a systematic way.

On the other hand, many important open problems in theoretical physics (such as the physics of low energy Quantum Chromo-Dynamics) are non-perturbative in nature. In particular, the Quantum Chromo-Dynamics (QCD henceforth) phase diagram and its finite density effects are quite challenging to analyze at non-perturbative level (see the nice reviews [51], [21], [32] and references therein). This circumstance makes mandatory to expand our knowledge of non-perturbative features of field theory.

This situation was perfectly understood by Freeman Dyson in his very famous two-page paper *Divergence of Perturbation Theory in Quantum Electrodynamics*

[43]. Dyson propose two possible alternatives in order to redress this problem. The Alternative A : there may be discovered a new method of carrying through the renormalization program, not making use of power series expansions. Alternative B : All the information that can in principle be obtained from the formalism of QFT is contained in the coefficients of the power series. In this case the observable are neither physically well-defined nor mathematically calculable, except in so far as the asymptotic expansions gives some workable approximation to it. In order to define the observable precisely, not merely new mathematical methods but a new physical theory is needed. Dyson itself recall the attractive features of alternative B because it would imply that quantum electrodynamics (and QFT in general) is in its mathematical nature not a closed theory.

Resurgence is one of the few theoretical techniques which can help to make sense of the ubiquitous factorially divergent series appearing in perturbation theory [65]. Such strategy works as follows: First of all, one must use Borel summation in the complex-g plane (g being the coupling constant of the theory) to handle the given factorially divergent series so that the divergent series becomes a finite expression. At a first glance, it seems that we have just traded one problem for another (maybe worse) problem since the Borel sum possesses ambiguities which manifest themselves along suitable lines in the complex g-plane (for nice reviews see [6] and [36]). However, when the models under investigation possess suitable topological charges labelling non-trivial non-perturbative sectors, the perturbative expansions in these topologically non-trivial sectors (which, usually, are also factorially divergent) allow a remarkable rescue. In these relevant theories, the ambiguities in the Borel summation of the perturbative expansions in the topologically non-trivial sectors cancel the ambiguities of the perturbative sector giving rise to a well-defined result [20], [99]. Starting from [63, 67] in recent years there has been a great revival of these ideas (see, for instance, [6], [36], [34], [100] and references therein) with applications in Quantum Mechanics, topological strings, and integrable Quantum Field Theory in low dimensions (see [34], [7], [4], [5], [41], [66], [62] and references therein)

The non-linear sigma model (NLSM henceforth) is one of the most interesting effective field theories. Besides the well-known relation with the low energy limit of QCD, such a model is also very useful in statistical mechanics, in the theory of the quantum hall effect, in the analysis of superfluids and so on (see [61], [13],

[45] and [68]). It is worth to emphasize that the NLSM on flat space-time does not possess static solutions with non-trivial topological charge due to Derrick's scaling argument [35]. A well-known method to avoid this no-go theorem was found by Skyrme (even before the actual paper of Derrick): the so-called Skyrme term [77] together with the NLSM allows the existence of static solitonic solutions with finite energy and topological charge, which represents the Baryonic charge, called Skyrmions (see [94], [14], [12], [2] and references therein). However, the original arguments in [94] to prove that the topological charge must be identified with the Baryon charge do not require explicitly the presence of the Skyrme term. Moreover, the Skyrme term is not the only way to avoid the Derrick's argument. The Derrick's scaling argument can be avoided by *constructing time-dependent ansatz for the matter fields with the characteristic that the corresponding energy-density is stationary.*

The gauged solitons constructed in [26] live at finite Baryon density and most of the energy and of the topological charge is contained within tube-shaped regions which are regularly spaced. These structures are expected in the description of cold and dense nuclear matter as a function of topological charge (commonly called *nuclear pasta*), and therefore are quite relevant in the phase diagram of the low energy limit of QCD (see [32] and [21]). Although until very recently the nuclear pasta phase was considered to be a very hard nut to crack from the analytic viewpoint, there are very strong observational evidences supporting it (see [54], [52], [53], [18] and references therein). The comparison of the energy density and Baryon density contour plots in [25], [26] and [27] with the ones in, for instance, [53] is very encouraging. Not only the analytic plots of energy density and Baryon density in [25], [26] and [27] are very close to the phenomenological ones in [54], [52], [53], [18], the present analytic framework also allows the explicit computation of relevant quantities (such as the computation of the shear modulus of the nuclear lasagna in [3] which is close to the value of the shear modulus of nuclear lasagna found in [28]).

On the other hand one of the most important types of plasma in plasma physics is the so-called Force Free Plasma (FFP henceforth). The study of force-free magnetic fields has its origin in astrophysics. For instance, objects with extremely intense magnetic fields like pulsars are typical sources of FFP. Also FFP has a key role in the so-called *Blandford-Znajek process* [19], mechanism that allows to

extract rotational energy from a spinning black hole. It is usually assumed that FFP is a plasma whose pressure is so small, relative to the magnetic pressure then that the plasma pressure may be ignored, and so only the magnetic pressure is considered.

The main goal of the present thesis is to study relevant physical properties of topologically non trivial gauged solitons and to use them to identify the proper resurgent parameters which in non-integrable theories are far from obvious. We use analytic solutions of the (3+1)-dimensional gauged non-linear sigma model representing crystals of gauged solitons at finite baryon density. Also we show that the electromagnetic field generated by the solitons crystals found in [25], [26] (which describe quite well many features of the *nuclear spaghetti phase*) is of force free type. In the present approach, the $SU(2)$ non-linear sigma model, which is the low limit of QCD describing Pions dynamic, provides with explicit and topologically non-trivial sources of FFP. This is in agreement with the fact that FFP must occur for objects made of hadronic matter.

The organization of the present thesis is as follow:

In chapter II we review the main aspects of resurgence theory. We define the basic concepts and study the canonical example of the Airy equation

Chapter III is devoted to present the origin and properties of crystals of gauged solitons in the non linear sigma model minimally coupled to Maxwell, the field equations and how to obtain both energy and topological charge, also we show that the electromagnetic field generated by the multi-solitons is a FFP.

In chapter IV we perform perturbations in the profile of the gauged solitons and electromagnetic perturbations. We show how we can use resurgence theory for the study of these fluctuations identifying resurgent parameters.

The last chapter is dedicated to the conclusions and final comments.

Chapter 2

Resurgence theory basics

Many problems in mathematics and physics are not solvable in closed form, and one has to resort to approximation schemes. Many of these approximations lead to formal power series in a small parameter which are generically divergent.

In the context of ODEs it is common to find solutions in terms of formal power series. However these series not always are analytic and moreover when one expand around a irregular point these series will be factorially divergent. Also perturbation theory in quantum mechanics in most of the cases gives as result series whose coefficients grow factorially. This situation is even worst in the context of quantum field theory in which expansion around instatons produce formal power series in $\hbar$ which in general are divergent.

It is crucial, both conceptually and technically, to make sense of these series. Based on the Jon Écalle work in [44] (see [33] [31] [71]), resurgence provides us with the only concrete hope to make sense of the deeply unpleasant feature of the perturbative approach in physics.

In this chapter we review the basic concepts to understand how resurgence theory works. This chapter is based on the excellent lecture notes by Marcos Mariño (see [64], [65]).

2.1 Basic Ingredients of Resurgence theory

Consider the formal power series

$$\varphi(z) = \sum_{n\geq 0} a_n z^n \tag{2.1.1}$$

it will be said that this series is asymptotic to the function $f(z)$, in the sense of Poincaré, if, for every N, the remainder after $N+1$ terms of the series is much smaller than the last retained term as $z \to 0$. This is,

$$\lim_{z\to 0} z^{-N}\left(f(z) - \sum_{n=0}^{N} a_n z^n\right) = 0 \tag{2.1.2}$$

Unlike convergent series in which we improve our approximation adding more terms for asymptotic series there exist a *optimal truncation* which give a good approximation. After a *optimal* N they will diverge. These series are the common objects in the context of perturbation theory.

The general symptom of the series in which we can apply resurgence are those in which the coefficients grows factorially

$$a_n \sim n! \tag{2.1.3}$$

In order to regularize this situation we need to use the Borel transform.

2.1.1 Borel Transform

Consider the following formal power series

$$\varphi(z) = \sum_{n\geq 0} a_n z^n \tag{2.1.4}$$

The Borel transform acts on formal power series as follows

$$\begin{aligned} \mathcal{B} : \mathbb{C}[[z]] &\to \mathbb{C}[[\zeta]], \\ z^n &\mapsto \zeta^n/n! \end{aligned} \tag{2.1.5}$$

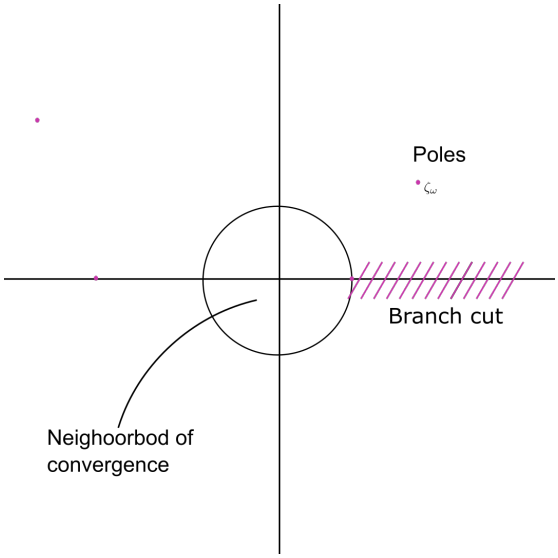

Figure 2.1.1: Borel ζ-plane. The zone of convergence delimited by the circumference

Therefore the Borel transform of (2.1.4) is given by

$$\widehat{\varphi}(\zeta) = \sum_{n\geq 0} a_n \frac{\zeta^n}{n!} \tag{2.1.6}$$

Remark 1: Using the Borel transform we obtain a new power series that It is convergent at the origin (in a neighborhood of origin) $\varphi(z) \to \widehat{\varphi}(\zeta)$. Outside the zone of convergence we can find all kind of singularities (poles, logarithmic, brunch cut, etc.) But, Why this structure is important? well the answer is that when you do a local expansion around this singularities (in the Borel ζ-plane) you will find new formal power series which at the beginning are invisible trough regular perturbation theory. Consider the following simple example for understand this point:

Example 1: Consider the serie $\varphi(z)$ and his borel transform given by $\widehat{\varphi}(\zeta)$. This series has a pole singularity ζ_ω in the Borel plane. We make a local expansion around this pole: $\zeta = \zeta_\omega + \xi$

The general structure of this local expansion is given by

$$\widehat{\varphi}\left(\zeta_\omega + \xi\right) = -\frac{a}{2\pi\xi} - \frac{1}{2\pi}\log(\xi)\sum_{n\geq 0}\widehat{c}_n\xi^n + \text{ regular terms} \tag{2.1.7}$$

Now, the next step is think about this new formal power series as the borel transform $\widehat{\varphi}_\omega(\xi)$ of a new formal power series $\varphi_\omega(z)$

$$\widehat{\varphi}_\omega(\xi) = \sum_{n\geq 0} \widehat{c}_n \xi^n \to \varphi_\omega(z) = \sum_{n\geq 0} c_n z^n \tag{2.1.8}$$

By this procedure one obtain a full family of formal power series

$$\varphi(z) \to \{\varphi_\omega(z)\}_\omega \tag{2.1.9}$$

Then the Borel transform can be use for obtain a big picture of the all pertubative sectors of our theory.

2.1.2 Borel resummation and Stokes rays

Let ζ_ω be a singularity of $\widehat{\varphi}(\zeta)$. A ray in the Borel plane which starts at origin and passes the through ζ_ω is called a Stokes ray. It is of the form $\mathrm{e}^{\mathrm{i}\theta}\mathbb{R}_+$, where $\theta = \arg(\zeta_\omega)$. Let $\varphi(z)$ a formal power series series, $z \in \mathbb{C}$, and $\theta = \arg z$. If $\widehat{\varphi}(\zeta)$ analytically continues to an L^1 -analytic function along the ray $\mathcal{C}^\theta := \mathrm{e}^{\mathrm{i}\theta}\mathbb{R}_+$ we define its Laplace transfrom by

$$s(\varphi)(z) = \int_0^\infty \widehat{\varphi}(z\zeta)\mathrm{e}^{-\zeta}\mathrm{d}\zeta = \frac{1}{z}\int_{\mathcal{C}^\theta} \widehat{\varphi}(\zeta)\mathrm{e}^{-\zeta/z}\,\mathrm{d}\zeta \tag{2.1.10}$$

The function $s(\varphi)(z)$ is often called the Borel resummation of the formal power series φ. The main motivation for this procedure is to pass from the world of formal power series to the world of functions. If $s(\varphi)(z)$ exists, its asymptotic behavior for small z can be obtained by expanding the integrand and integrating term by term:

$$s(\varphi)(z) \sim \sum_{n\geq 0} a_n z^n \tag{2.1.11}$$

This is the formal power series that we started with.

But if $\arg(\zeta) = \theta$ is the argument of a Stokes ray we need to avoid the singularity trough contour deformation. This is the so called *Lateral Borel Resummation* and is defined by

$$s_\pm(\varphi)(z) = \frac{1}{z}\int_{\mathcal{C}^\theta_\pm} \widehat{\varphi}(\zeta)\mathrm{e}^{-\zeta/z}\,\mathrm{d}\zeta \tag{2.1.12}$$

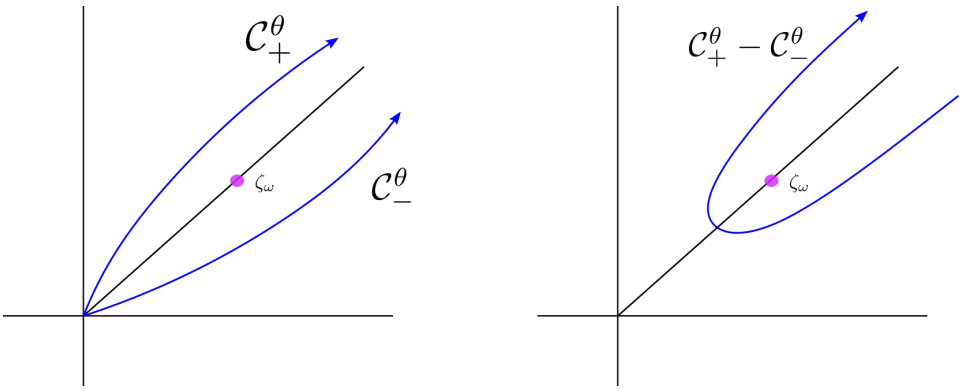

Figure 2.1.2: Contour deformation in the calculation of the discontinuity.

The discontinuity produced by one singularity is simply given by

$$s_+(\varphi)(z) - s_-(\varphi)(z) = \mathrm{i}\mathrm{e}^{-\zeta_\omega/z} s_-\left(\varphi_\omega\right)(z) \tag{2.1.13}$$

More generally, if there are many singularities, we find

$$s_+\left(\varphi_\omega\right)(z) - s_-\left(\varphi_\omega\right)(z) = \mathrm{i}\sum_{\omega'} \mathrm{S}_{\omega\omega'} \mathrm{e}^{-\zeta_{\omega'}/z} s_-\left(\varphi_{\omega'}\right)(z) \tag{2.1.14}$$

The natural object that appears in the right hand side of the last expression is a *formal linear combination of a family of formal power series*. Formally this objects are defined as Trans-series and they encoded all the perturbative sectors of a given theory.

2.1.3 Trans-series

One of the most important implications of resurgence is that, in order to reconstruct actual functions through Borel resummation, we need, in addition to the "starting" perturbative series, all additional series $\varphi_\omega(z)$ appearing in the resurgent structure. A trans-series is a formal linear combination of formal power series.

$$\Phi(z;\vec{C}) = \sum_\omega C_\omega \mathrm{e}^{-\zeta_\omega/z} \varphi_\omega(z) \tag{2.1.15}$$

where $\vec{C} = (C_{\omega_1}, \cdots)$ is a vector of complex numbers. Note that the trans-series is fully determined by the terms C_ω and $-\zeta_\omega/z$ which are called *trans-series parameters*.

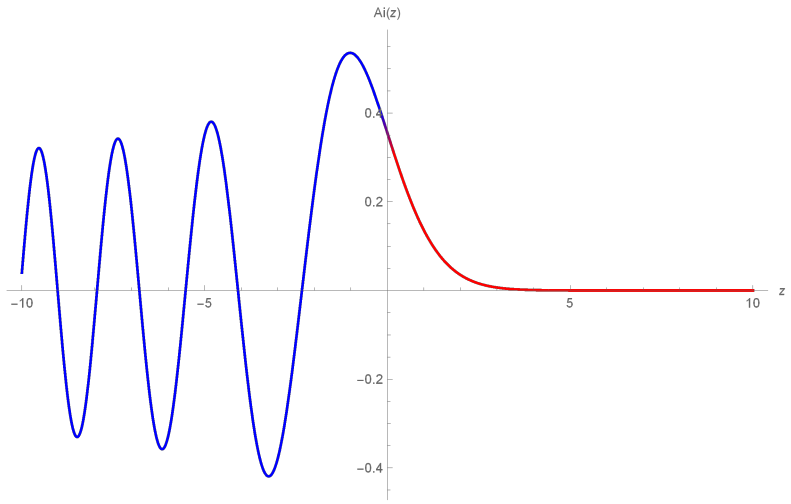

Figure 2.2.1: Plot of the Airy function $\mathrm{Ai}(z)$ as a function of z. We put in blue the oscillatory behaviour for $z < 0$ and in red exponentially suppress behaviour for $z > 0$

Trans-series are, in a sense, the most general object that one is forced to consider in the theory of resurgence. The hope of resurgence is to be able to reconstruct as much is possible from trans-series. In general the expectation in the context of resurgence theory is that the functions that we want to reconstruct are lateral Borel resummations of trans-series.

$$S_{\pm}(\Phi)(z) = \sum_{\omega} C_{\omega} e^{-\zeta_{\omega}/z} S_{\pm}\left(\varphi_{\omega}\right)(z) \tag{2.1.16}$$

2.2 Canonical Example: Airy Equation

The Airy equation is given by

$$y''(z) - zy(z) = 0 \tag{2.2.1}$$

This equation has two linear independent solutions: the Airy functions $\mathrm{Ai}(z)$ and $\mathrm{Bi}(z)$ (sometimes calls Airy function of the second kind). We plot $\mathrm{Ai}(z)$ the in Fig. 2.2.1. Then the general solution to the Eq. (2.2.1) is given by

$$y(z) = c_1 \mathrm{Ai}(z) + c_2 \mathrm{Bi}(z) \tag{2.2.2}$$

But we are now interested in formal power series solutions to this equation. Many softwares have functions that perform asymptotic expansions, for example using Mathematica we obtain the first three terms of the asymptotic solutions around $z = +\infty$

$$\begin{aligned} y(z) \approx c_1 e^{-\frac{2z^{3/2}}{3}} 2z^{3/2} \left(-\frac{5}{48z^{7/4}} + \frac{385}{4608z^{13/4}} + \frac{1}{\sqrt[4]{z}} + \dots \right) \\ + c_2 e^{\frac{2z^{3/2}}{3}} \left(\frac{5}{48z^{7/4}} + \frac{385}{4608z^{13/4}} + \frac{1}{\sqrt[4]{z}} + \dots \right) \end{aligned}$$

From classic asymptotic theory the asymptotic expansion of the Airy functions are given by

$$\mathrm{Ai}(x) \sim \frac{1}{2x^{1/4}\sqrt{\pi}} \mathrm{e}^{-2x^{3/2}/3} \varphi_1(z), \quad z = x^{-3/2}, \qquad x >> 1 \tag{2.2.3}$$

$$\mathrm{Bi}(x) \sim \frac{1}{2x^{1/4}\sqrt{\pi}} \mathrm{e}^{2x^{3/2}/3} \varphi_2(z), \quad z = x^{-3/2}, \qquad x >> 1 \tag{2.2.4}$$

where

$$\begin{aligned} \varphi_{1,2}(z) &= \sum_{n=0}^{\infty} \frac{1}{2\pi} \left(\mp \frac{3}{4} \right)^n \frac{\Gamma\left(n + \frac{5}{6}\right) \Gamma\left(n + \frac{1}{6}\right)}{n!} z^n \\ &= 1 \pm \frac{5}{48} z + \frac{385}{4608} z^2 \pm \frac{85085}{663552} z^3 + \cdots \end{aligned} \tag{2.2.5}$$

Now trough the eyes of resurgence the asymptotic definitions of the Airy function has a more powerful meaning and we promote the asymptotic statement to an exact statement.

From here we want to show the resurgence structure of this simple function. Our starting point it's going to be a formal power series whose coefficients are given by (2.2.5)

$$\varphi_1(z) = \sum_{n=0}^{\infty} \frac{1}{2\pi} \left(-\frac{3}{4} \right)^n \frac{\Gamma\left(n + \frac{5}{6}\right) \Gamma\left(n + \frac{1}{6}\right)}{n!} z^n \tag{2.2.6}$$

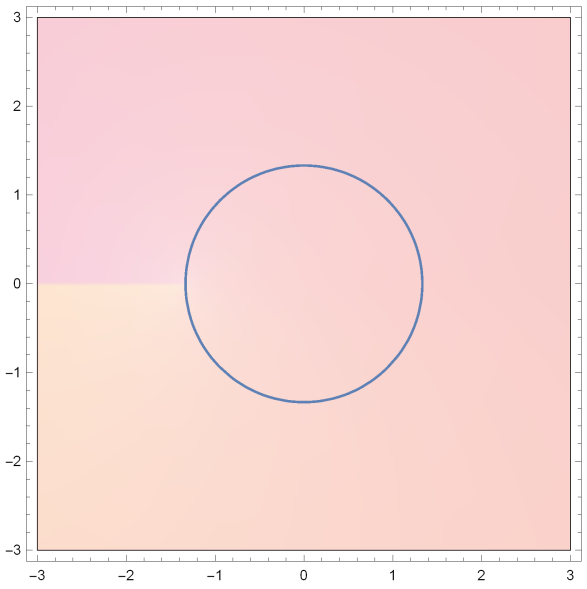

Figure 2.2.2: Borel ζ-plane. The zone of convergence delimited by the blue circumference and the logarithmic singularity at $\zeta = -4/3$

After the Borel transform we obtain a close expression[1] in terms of a hypergeometric function.

$$\widehat{\varphi}_1(\zeta) = \frac{\Gamma\left(\frac{1}{6}\right)\Gamma\left(\frac{5}{6}\right)\,{}_2F_1\left(\frac{1}{6},\frac{5}{6};1;-\frac{1}{4}(3\zeta)\right)}{2\pi} \tag{2.2.7}$$

This function is analytic at the origin in a region delimited by the condition

$${}_2F_1\left(\frac{1}{6},\frac{5}{6};1;-\frac{1}{4}(3z)\right) = 0$$

It is easy to see from the plot of the Borel transform in Fig. 2.2.2 that there is a singularity at $\zeta = -4/3$ just next to the zone of convergence

From the general theory of hypergeometric functions we know that the singularity is of logarithmic type, and one finds

$$\widehat{\varphi}(-4/3+\xi) = -\frac{1}{2\pi}\log(\xi)\,{}_2F_1\left(\frac{1}{6},\frac{5}{6},1;\frac{3\zeta}{4}\right) + \text{regular terms} \tag{2.2.8}$$

Inmediately we identify this new series as the Borel transform of $\varphi_2(z) := \varphi_{-4/3}(z)$ whose coefficients are given by $\varphi_2(z)$ in (2.2.5). Now we can understand the origin

[1] It is worth to mention that this situation is kind of luxury and in most of the cases there is not a close expression for the Borel transform.

of the name "resurgence": the other solution of the Airy Eq. resurge from the asymptotic solution of the other.

Now, we can improve the asymptotic statement in 2.2.3 by means of an exact statement. To reconstruct the Airy function $\mathrm{Ai}(x)$ out of Borel resummations of the formal power series $\varphi_{1,2}(z)$ it will depends on the argument of x.

$$\mathrm{Ai}(x) = \frac{1}{2x^{1/4}\sqrt{\pi}} \mathrm{e}^{-2x^{3/2}/3} S(\varphi_1)(z), \quad |\arg(x)| < 2\pi/3 \tag{2.2.9}$$

$$\mathrm{Ai}(x) = \frac{1}{2x^{1/4}\sqrt{\pi}} \left\{ \mathrm{e}^{-2x^{3/2}/3} s\left(\varphi_1\right)(z) + i\mathrm{e}^{2x^{3/2}/3} s\left(\varphi_2\right)(z) \right\}, \quad |\arg(x) - \pi| < \pi/3 \tag{2.2.10}$$

This leads to the well-known oscillatory behavior of the Airy function along the negative real axis,

$$\mathrm{Ai}(-x) \sim \frac{x^{-1/4}}{\sqrt{\pi}} \cos\left(\frac{2}{3}x^{3/2} - \frac{\pi}{4}\right), \quad x \to \infty \tag{2.2.11}$$

2.2.1 Integral representation of the Airy function

Applying the Fourier transform to the Eq. (2.2.1) we obtain

$$-t^2\hat{y}(t) - i\hat{y}'(t) = 0 \tag{2.2.12}$$

then

$$\hat{y}(t) = Ce^{it^3/3} \tag{2.2.13}$$

where C is an arbitrary constant of integration. The inverse transform is

$$y(z) = \frac{C}{2\pi} \int_{-\infty}^{\infty} dt \exp\left(i\left[zt + t^3/3\right]\right) \tag{2.2.14}$$

The integral representation of the Airy function Ai is given by the choice $C = 1$ then

$$\mathrm{Ai}(z) = \frac{1}{2\pi} \int_{-\infty}^{\infty} dt \exp\left(\frac{1i}{3}t^3 + izt\right), \quad z \in \mathbb{C} \tag{2.2.15}$$

The leading term in the asymptotic expansion of (2.2.15) is given by

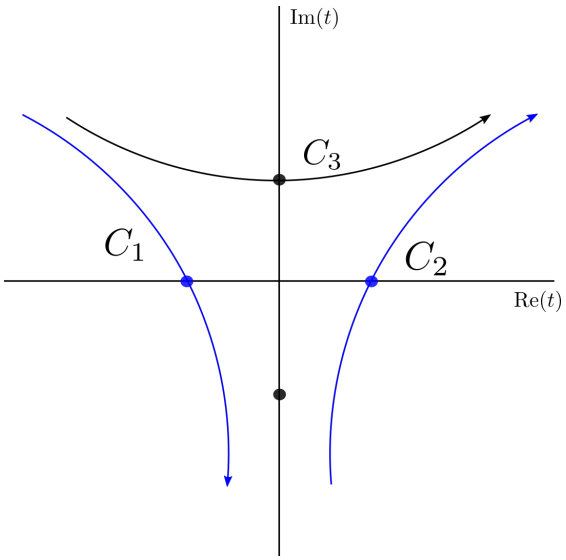

Figure 2.2.3: Steepest descent contours for Ai(z) in complex t plane. There are two saddles for any z, given by $t^2 + z = 0$. Blue (black) dots show locations of saddles for negative (positive) z. For $z < 0$, both saddles contribute through contours C_1 and C_2. For $z > 0$, only one saddle contributes, via contour C_3.

$$\text{Ai}(z) \sim \begin{cases} \frac{1}{2\sqrt{\pi} z^{1/4}} \exp\left(-\frac{2}{3} z^{\frac{3}{2}}\right), & z \to \infty \\ \frac{1}{\sqrt{\pi}(-z)^{1/4}} \sin\left(\frac{2}{3}(-z)^{\frac{3}{2}} + \frac{\pi}{4}\right), & z \to -\infty \end{cases} \tag{2.2.16}$$

There are two very different asymptotic behaviors even though they are both derived from the integral which is valid throughout the complex plane. We can see in the Fig. 2.2.1 the oscillatory behaviour for $z < 0$ and exponential suppressed behaviour for $z > 0$. To understand this situation it is convenient use the steepest descend method in order to perform the integral.

By looking at the saddles of the argument of the exponential in (2.2.15) in the complex t plane. There are two saddles, given by $t^2 + z = 0$. When z is on the real positive line, the saddles are purely imaginary, $\pm i\sqrt{z}$. As z decreases and approaches the origin, the saddles too move closer to the origin until they become exactly zero. When z moves to the real negative line, the saddles separate out again and become real, $\pm\sqrt{-z}$. Depending on the phase of z, the steepest descent contour may pass through only one of the saddles. As the phase of z changes, the contour moves around in the complex plane and at $z = 0-$ it goes through both the saddles (see Fig. 2.2.3). This phenomena is called the Stokes phenomena, where saddles exchange (acquire) dominance as we change the phase of z, and it motivates us to write the asymptotic of the Airy function as a single expression:

$$\mathrm{Ai}(z) \sim \frac{1}{2\sqrt{\pi} z^{1/4}} e^{-\frac{2}{3} z^{\frac{3}{2}}} + C e^{i\pi/4} \frac{1}{2\sqrt{\pi} z^{1/4}} e^{\frac{2}{3} z^{\frac{3}{2}}} \tag{2.2.17}$$

where C is the Stokes parameter. It controls the dominance of the saddles (Stokes phenomenon) and is an implicit function of the phase of z. From this expression we recover the exact statement in Eq. (2.2.10).

2.3 Resurgence in Physics

From a historically point of view many of the ideas of resurgence were seen before of *Ecalle resurgence theory* (see for example [17], [89], [56]). In these previous works physicists related large order behavior of perturbative series's coefficients with leading instanton terms. Bogomolny and Zinn-Justin ([20], [98]) showed that the imaginary part arising from the Borel summation of perturbative expansion of the ground state energy in certain quantum mechanical models cancels exactly with the 1-instanton contribution. This almost miraculous cancellation is one of the core features of resurgence theory.

Resurgence theory has been applied successfully to many quantum mechanical models (see for example [15], [8], [39], [40]). An important application of resurgence in this context is to the WKB method which is then upgraded to the so-called "exact WKB method" or "all orders WKB method" (see [78] [40]). One the most illustrative examples of resurgence in QM is the case of the Schrödinger equation for the periodic cosine (Mathieu) potential [41].

$$-\frac{\hbar^2}{2}\frac{d^2}{dx^2}\psi(x) + \cos(x)\psi(x) = u\psi(x) \tag{2.3.1}$$

In this case it is known that standard Rayleigh-Schrödinger perturbation theory leads to a perturbative series that is divergent. This situation can be remedied by recognizing that the full expansion of the energy at small coupling is in fact of the "trans-series" form:

$$u_{\text{trans}}(\hbar, N) = \sum_{k=0}^{\infty}\sum_{n=0}^{\infty}\sum_{l=1}^{k-1} c_{k,n,l}(N)\hbar^n \left(\frac{1}{\hbar^{N+1/2}}\exp\left[-\frac{S}{\hbar}\right]\right)^k \left(\ln\left[-\frac{1}{\hbar}\right]\right)^l \tag{2.3.2}$$

Note that in such case is obvious that $\hbar$ is a resurgent parameter in the trans-

series. A very important step in the application of resurgence to physics is the identification of a *proper resurgent parameter*. This step usually assumed to be obvious since in all the known solvable cases the resurgent parameter is the coupling constant. However in non-integrable theories at finite volume this step is far from obvious since seems many different choice of parameter may be available. In the case of the gauged soliton that we study in this thesis the resurgent parameter doesn't depend on the coupling constant of the theory (NLSM).

In QFT the procedure of resurgence is not so straightforward. Nevertheless many important results about resurgence in QFT exist (see [42], [37], [38]). For example, resurgence theory was used to prove the existence of non-perturbative features in deformations of the 2D principal chiral model ([72]). The last example shares some characteristics with the work presented in this thesis in the sense that in reference [72] using dimensional reduction they go from the complete QFT to a Schrödinger equation with elliptical potential and for such potential they study the ground state energy using resurgence. As we will see in Chapter IV, the perturbations to gauged solitons in (3+1)-dimensions presented in the next chapter are characterized by elliptical potentials in one dimension.

Chapter 3

Crystal structures in the (3+1)-D gauged non-linear sigma model

One of the most relevant field theories (both due to its predictive power as well as its non-trivial topological features) is the non-linear sigma model minimally coupled to Maxwell. It is a very effective tool from high energy physics to statistical mechanics systems like quantum magnetism, the quantum hall effect, meson interactions, superfluid. He and string theory (see [60] [13]) it was introduced in particle physics to describe the low-energy dynamics of pions (see for instance [45], [68] and references therein).

In this section we will study the construction of solutions that describe multi-solitons charged within a finite volume. These configurations are allowed when the Skyrme term vanishes. Within this formalism we will also include a mass term.

The solitons that we will consider here are static, in the sense that the energy density (or more generally, its energy-momentum tensor) does not depend on time, even though the U field explicitly depends on this coordinate, as we will see below.

3.1 The action of the gauged Non-Linear Sigma model

The action of the $U(1)$ gauged Non-Linear Sigma model (NLSM henceforth) minimally coupled with Maxwell theory is

$$S = \int d^4x\sqrt{-g}\left[\frac{K}{4}\mathrm{Tr}\left(L^\mu L_\mu\right) - m^2\mathrm{Tr}\left(U+U^{-1}\right) - \frac{1}{4}F_{\mu\nu}F^{\mu\nu}\right] \ , \tag{3.1.1}$$

$$L_\mu = U^{-1}D_\mu U \ , \quad D_\mu = \nabla_\mu + A_\mu\left[t_3, \ .\ \right] \ , \tag{3.1.2}$$

$$U \in SU(2) \ , \quad L_\mu = L^j_\mu t_j \ , \quad t_j = i\sigma_j \ , \ F_{\mu\nu} = \partial_\mu A_\nu - \partial_\nu A_\mu \ , \tag{3.1.3}$$

where $\sqrt{-g}$ is the (square root of minus) the determinant of the metric, m is the Pions mass, K is the coupling constant of the NLSM, A_μ is the gauge potential, ∇_μ is the partial derivative and σ_i are the Pauli matrices.

The energy-momentum tensor of the model is

$$T_{\mu\nu} = -\frac{K}{2}\mathrm{Tr}\left[L_\mu L_\nu - \frac{1}{2}g_{\mu\nu}L^\alpha L_\alpha\right] - m^2\mathrm{Tr}\left[g_{\mu\nu}(U+U^{-1})\right] + \bar{T}_{\mu\nu} \ ,$$

with

$$\bar{T}_{\mu\nu} = F_{\mu\alpha}F_\nu{}^\alpha - \frac{1}{4}F_{\alpha\beta}F^{\alpha\beta}g_{\mu\nu} \ , \tag{3.1.4}$$

being the electromagnetic energy-momentum tensor.

The field equations are

$$D_\mu L^\mu + \frac{2m^2}{K}\left(U - U^{-1}\right) = 0 \ , \tag{3.1.5}$$

$$\nabla_\mu F^{\mu\nu} = J^\nu \ , \tag{3.1.6}$$

where the current J^μ is given by

$$J^\mu = \frac{K}{2}\mathrm{Tr}\left[\widehat{O}L^\mu\right] \ , \qquad \widehat{O} = U^{-1}t_3U - t_3 \ . \tag{3.1.7}$$

On the other hand the correct expression for the topological charge of the gauged non-linear sigma model has been constructed in [24] (see also the pedagogical

analysis in [70]):

$$B = \frac{1}{24\pi^2}\int_{\Sigma}\rho_B \ , \tag{3.1.8}$$

where

$$\rho_B = \epsilon^{ijk}\mathrm{Tr}\Big[\left(U^{-1}\partial_i U\right)\left(U^{-1}\partial_j U\right)\left(U^{-1}\partial_k U\right) - \partial_i\left[3A_j t_3\left(U^{-1}\partial_k U + \left(\partial_k U\right)U^{-1}\right)\right]\Big] \ . \tag{3.1.9}$$

Note that the second term in Eq. (3.1.9) guarantees both the conservation and the gauge invariance of the topological charge. When Σ is space-like, B is the baryon charge of the configuration.

3.2 Gauged crystals

3.2.1 Te ansatz

As it has been already emphasized, the analytic description of cold and dense nuclear matter as a function of topological charge is a very interesting but quite chalenging theoretical problem (see [32] [21] and references therein). Since one of the main goals of the present analysis is precisely to understand how gauged solitons react to the presence of a finite volume containing them, we need to analyze the model in the following flat metric

$$ds^2 = -dt^2 + L_r^2 dr^2 + L_\theta^2 d\theta^2 + L^2 d\phi^2 \ .$$

where $4\pi^3 L_r L_\theta L$ is the volume of the box in which the gauged solitons are confined. The adimensional coordinates r, θ and ϕ have the ranges

$$0 \leq r \leq 2\pi, \quad 0 \leq \theta \leq \pi, \quad 0 \leq \phi \leq 2\pi \tag{3.2.1}$$

For the U field we adopt the standard parametrization of an element of $SU(2)$, that is

$$U^{\pm 1}\left(x^\mu\right) = \cos(\alpha)\mathbf{1}_2 \pm \sin(\alpha) n^i t_i \ , \tag{3.2.2}$$

where $\mathbf{1}_2$ is the 2×2 identity matrix and

$$n^1 = \sin\Theta\cos\Phi, \quad n^2 = \sin\Theta\sin\Phi, \quad n^3 = \cos\Theta \ , \tag{3.2.3}$$
$$\alpha = \alpha(x^\mu) \ , \quad \Theta = \Theta(x^\mu) \ , \quad \Phi = \Phi(x^\mu) \ , \quad n^i n_i = 1 \ .$$

Because we want to construct analytical solutions, it is necessary to have a good ansatz that significantly reduces the field equations in Eqs. (3.1.5) and (3.1.6). The approach developed in [25], [26] and [27] lead to the following ansatz for the gauged solitons

$$\alpha = \alpha(r), \Theta = q\theta, \Phi = p\left(\frac{t}{L} - \phi\right), q = 2v+1, \quad p, v \in \mathbb{N}, p \neq 0 \tag{3.2.4}$$

as well as for the electromagnetic potential

$$A_\mu = (u(r,\theta), 0, 0, -Lu(r,\theta)) \tag{3.2.5}$$

It is a direct computation to verify that the ansatz defined in Eqs. (3.2.4) and (3.2.5) possesses the "hedgehog property". Such a property, which in the past was usually only associated to spherically symmetric solitons, corresponds to the following desirable feature: one would like to reduce the coupled system of non-linear field equations defining the solitons to only one non-linear equation for the profile keeping alive the topological charge. In the present case, quite remarkably, this property holds despite the lack of spherical symmetry and despite the minimal coupling with the Maxwell gauge field, as we will see below.

3.2.2 Field equations

Using the ansatz in Eqs. (3.2.4) and (3.2.5) one can check directly that *first of all* the three coupled field equations of the gauged NLSM reduce to a single ODE for the profile α:

$$\alpha'' - \frac{q^2}{2}\frac{L_r^2}{L_\theta^2}\sin(2\alpha) + \frac{4L_r^2 m^2}{K}\sin(\alpha) \ = \ 0$$

We can note one of the main features of our ansatz is that the $U(1)$ gauged potential does not enter explicitly in the field equations. The ansatz allows to decouple Eqs. (3.1.5) and (3.1.6) and thanks to the following relations:

$$A_\mu A^\mu = 0, \quad (\nabla_\mu \Phi)(\nabla^\mu \Phi) = 0, \quad A_\mu \nabla^\mu \Phi = 0$$

$$(\nabla_\mu \Theta)(\nabla^\mu \Phi) = 0, \quad A_\mu \nabla^\mu \Theta = 0, \quad A_\mu \nabla^\mu \alpha = 0$$

one can first solve the equation of the gauged non-linear sigma model explicitly. Then, once the $SU(2)$ valued scalar field is known, the Maxwell equations reduce to a linear equation in which the soliton plays the role of an effective potential.

Eq. (3.2.2) can be integrated easily in terms of inverse elliptic functions observing that it is equivalent to the following first order equation

$$\alpha' = \pm \left[2 \left(E_0 - \frac{q^2}{4} \frac{L_r^2}{L_\theta^2} \cos(2\alpha) + \frac{4m^2 L_r^2}{K} \cos(\alpha) \right) \right]^{1/2} \quad \Rightarrow \tag{3.2.6}$$

$$\pm dr = \frac{d\alpha}{\left[2 \left(E_0 - \frac{q^2}{4} \frac{L_r^2}{L_\theta^2} \cos(2\alpha) + \frac{4m^2 L_r^2}{K} \cos(\alpha) \right) \right]^{1/2}} , \tag{3.2.7}$$

(E_0 being an integration constant). The above equation (3.2.7) can be integrated in terms of inverse elliptic functions. A necessary condition for stability is that α' does not change sign so that we must require

$$E_0 > \frac{q^2}{4} \frac{L_r^2}{L_\theta^2} + \frac{4m^2}{K} L_r^2 . \tag{3.2.8}$$

The integration constant E_0 is fixed in terms of n through the relation

$$n \int_0^\pi \frac{1}{\eta(n\alpha, E_0)} d\alpha = 2\pi, \tag{3.2.9}$$

$$\eta(\alpha, E_0) = \pm \left[2 \left(E_0 - \frac{q^2}{4} \frac{L_r^2}{L_\theta^2} \cos(2\alpha) + \frac{4m^2 L_r^2}{K} \cos(\alpha) \right) \right]^{1/2} \tag{3.2.10}$$

Secondly, the Maxwell equations are reduced to just one linear Schrodinger-like equation with an effective two-dimensional potential which can be found explicitly in terms of the soliton profile:

$$\Delta u + V u = \sigma ,$$

$$V = \frac{2L_\phi}{p} \sigma , \quad \sigma = \frac{2Kp}{L} \sin^2(\alpha) \sin^2(q\theta) .$$

Defining

$$\Psi = \frac{2L}{p}u - 1 \ ,$$

the Maxwell equation becomes

$$\Delta\Psi + V\Psi \ = \ 0 \ , \qquad \Delta \equiv \frac{1}{L_r^2}\partial_r^2 + \frac{1}{L_\theta^2}\partial_\theta^2 \ .$$

3.2.3 Topological charge and energy density

According to Eqs. (3.1.8), (3.2.2) and (3.2.3) it follows that the topological charge density is

$$\rho_{\rm B} = 12(\sin^2\alpha\sin\Theta)\ d\alpha\wedge d\Theta\wedge d\Phi \ . \tag{3.2.11}$$

The topological density for the configurations here constructed, read

$$\rho_B = \rho_B^{\rm NLSM} + \rho_B^{\rm Maxwell} \tag{3.2.12}$$

where

$$\begin{aligned}\rho_B^{\rm NLSM} &= -12pq\sin(q\theta)\sin^2(\alpha)\partial_r\alpha \\ \rho_B^{\rm Maxwell} &= 12L\left[\left(2q\sin(q\theta)\sin^2(\alpha)u - \cos(q\theta)\partial_\theta u\right)\partial_r\alpha - q\sin(\alpha)\cos(\alpha)\sin(q\theta)\partial_r u\right]\end{aligned} \tag{3.2.13}$$

which can be also written as

$$\rho_B = 3q\frac{\partial}{\partial r}(p\sin(q\theta)(\sin(2\alpha)-2\alpha) - 2L\sin(q\theta)u\sin(2\alpha)) - \frac{\partial}{\partial\theta}\left(12L\alpha' u\cos(q\theta)\right) \tag{3.2.14}$$

Thus, we can read the boundary conditions for the fields:

$$\alpha(2\pi) - \alpha(0) = n\pi \tag{3.2.15}$$

and with this the topological charge becomes

$$W = -np\times\left(\frac{1-(-1)^q}{2}\right) - \frac{L}{\pi}\int_0^{2\pi} dr\alpha'\left((-1)^q u(r,\pi) - u(r,0)\right) \tag{3.2.16}$$

If we assume a boundary condition for u given by

$$u(r,\pi) = (-1)^q u(r,0) \tag{3.2.17}$$

we obtain

$$W = \begin{cases} -np & \text{if} \quad q \in 2\mathbb{Z}+1 \\ 0 & \text{if} \quad q \in 2\mathbb{Z} \end{cases} \tag{3.2.18}$$

On the other hand, the energy-density is

$$\begin{aligned} T_{00} &= \frac{K}{2L_r^2 L_\theta^2 L^2}\left(L_\theta^2 L^2 \alpha'^2 + 2L_r^2 \sin^2(\alpha)\left[L^2 q^2 + 2L_\theta^2 \sin^2(q\theta)(p-2Lu)^2\right]\right) \\ &\quad + 4m^2\cos(\alpha) + \frac{1}{L_r^2}(\partial_r u)^2 + \frac{1}{L_\theta^2}(\partial_\theta u)^2 \ . \end{aligned} \tag{3.2.19}$$

It is also convenient (as it will be explained in the next sections) to define the "reduced energy density ε_r in the r-direction" obtained integrating Eq. (3.2.19) along the θ and ϕ:

$$\varepsilon_r = \int (L_\theta L)\, T_{00} d\theta d\phi \ . \tag{3.2.20}$$

This reduced energy density represents the effective energy density (namely, the energy per unit of length) in the r-direction and can be compared directly with 1-dimensional model possessing solitons crystals. In the particular case in which both the Maxwell gauge potential and the Pions mass vanish one gets

$$\varepsilon_r^{(0)} = \varepsilon_r(u=0, m=0) \ , \tag{3.2.21}$$

$$\varepsilon_r^{(0)} = \frac{\pi K}{L_r^2 L_\theta L}\int d\theta \left(L_\theta^2 L^2 \alpha'^2 + 2L_r^2 \sin^2(\alpha)\left[L^2 q^2 + 2L_\theta^2 \sin^2(q\theta)p^2\right]\right) \ . \tag{3.2.22}$$

$$\varepsilon_r^{(0)} = \frac{\pi K \sin^2(\alpha(r))\left(2\pi q\left(L^2 q^2 + L_\theta^2 p^2\right) - L_\theta^2 p^2 \sin(2\pi q)\right)}{L L_\theta q} + \frac{\pi^2 K L L_\theta \alpha'^2}{L_r^2} \ . \tag{3.2.23}$$

Figure 3.2.1 shows the energy density of different configurations for a given value of the topological charge ($B = 5$ in this case) when the parameters q and m changes. For this we have imposed the boundary conditions $u(r,0) = u(r,\pi) = 0$. One can see that, as the value of q increases, the peaks become more localized and their intensity also increases. On the other hand, when the value of the mass becomes larger, it is observed that the spacing between the tubes in the r direction becomes irregular, in such a way that the tubes are grouped in pairs in this direction.

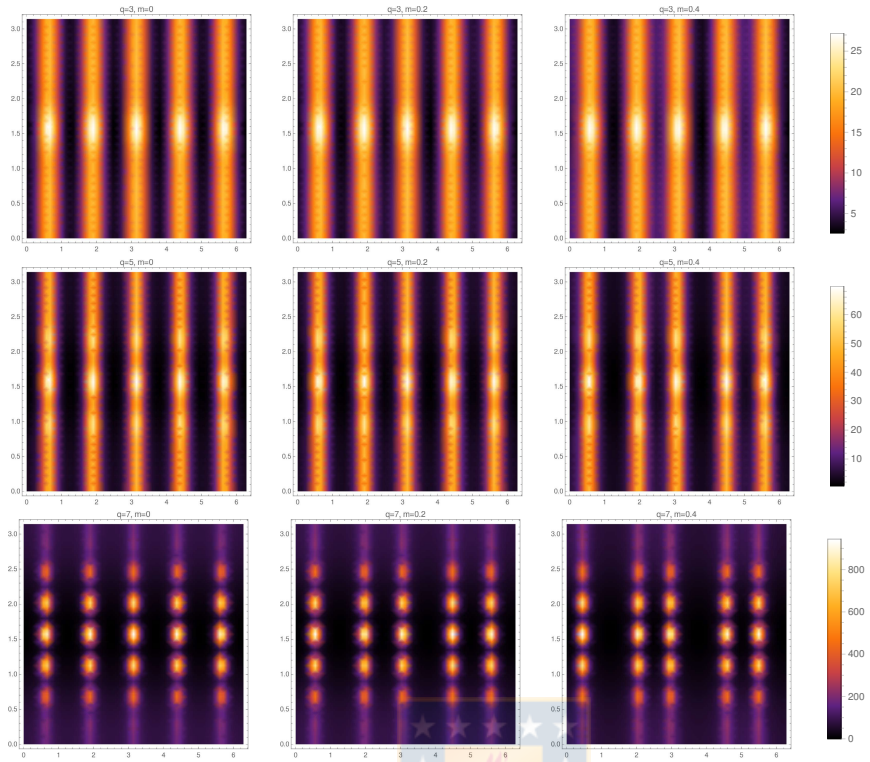

Figure 3.2.1: Comparison of the energy density for different configurations with topological charge $B = 5$, as function of q and m. Here we have considered $n = 5$, $K = 2$, $L = 1$ and $p = 1$.

3.3 Force Free Plasma Condition

One of the most important types of plasma in plasma physics is the so-called Force Free Plasma (FFP henceforth), and several reasons justify this statement. First of all, FFP are extremely relevant in many astrophysical situations. For instance, objects with extremely intense magnetic fields like pulsars are typical sources of FFP. Secondly, FFP can be characterized in a very elegant way with a non-linear set of PDEs for the electromagnetic field. This is the so-called force free condition,

$$F_{\mu\nu}\nabla_\rho F^{\nu\rho} = 0 \ . \tag{3.3.1}$$

The above equation is usually the starting point of the theoretical analysis on FFP (see for instance [93], [92] and references therein). From one point of view, the above system of equations is very convenient since many features of FFP can be analyzed without taking into account the electromagnetic sources (which are absent in Eq. (3.3.1)). On the other hand, this implies that often the very

important physical question about which are the actual concrete sources able to generate such FFP is somehow neglected. In the present chapter, as it will be explained in the following sections, we identify a very natural and concrete source of FFP in the low energy limit of Quantum Chromodynamics (QCD). FFP play also a key role in the so-called *Blandford-Znajek process* [19], mechanism that allows to extract rotational energy from a spinning black hole. This happens when the electric potential becomes larger than the threshold of electron-positron pair creation, so that the black hole will be surrounded by an FFP in such a way that the rotation energy can be radiated away. The pioneering theoretical analysis in [59], [84], [85], [86], [87], [88], [55] and [48] shed considerable light on this process.

In recent years relevant analytic examples of FFP have been constructed (see, for instance, [23], [58], [22], [95], [96], [57], [97], [49], [30], [50] and references therein), however, many of the available examples (which analyze in detail solutions of the system in Eq. (3.3.1)) leave open the issue to identify the actual sources of the force-free electromagnetic field. Due to the interesting astrophysical applications of FFP it is of great importance to find also analytic examples of FFP in which the sources of the electromagnetic field can be traced back directly to observed particles of the standard model.

3.3.1 Emergent force free plasma

The force free condition

$$F_{\mu\nu}\nabla_{\rho}F^{\nu\rho} = 0 \ , \tag{3.3.2}$$

is realized in many relevant examples of plasmas such as in the solar corona [93] or close to rotating neutron stars and black holes [46], [69], [47]. As it was already mentioned the FFP plays an important role in the Blandford-Znajek process [19] but, even in such process, the FFP emerge as a suitable choice that "provide a reasonable approximation to the time-averaged structure of the magnetosphere", and then, the black hole parameters are estimate values in order to satisfy the force-free condition.

It can be readily seen that the Maxwell field surrounding our gauged solitons satisfies the force-free condition in Eq. (3.3.2). First, note that the $U(1)$ gauge

potential in Eq. (3.2.5) can be written as

$$A_\mu dx^\mu = u(r,\theta)\,(dt - Ld\phi) \ ,$$

so that the field strength is found to be

$$F_{\mu\nu} = ((\partial_r u)\,dr + (\partial_\theta u)\,d\theta) \wedge (dt - Ld\phi) \ .$$

It follows that the divergence of the field strength, identified with the current, is

$$J^\nu = \nabla_\mu F^{\mu\nu} = c_1 \sin^2(\alpha)\sin^2(q\theta)\,(\partial^\mu \Phi - c_2 A^\mu) \ ,$$
$$\text{with} \qquad c_1 = -\frac{2K}{L}, \quad c_2 = 2L \ ,$$

which is manifestly orthogonal to the field strength $F_{\mu\nu}$. Therefore we see that the force-free condition in Eq. (3.3.2) is automatically satisfied.

The electromagnetic field lines (for suitable choice of the parameters) are presented in Fig. 3.3.2, where we have used the following boundary conditions for the Maxwell potential

$$u(r,0) = u(r,\pi) = 0 \ , \quad u(0,r) = u(2\pi,0) = 0 \ . \tag{3.3.3}$$

At this point it is important to emphasize that, although several analytic solutions to the force-free Maxwell equations could be found (for instance, using the approaches in [23], [22], [95], [96], [97], [49] and [30]) most of these analytic solutions to the force-free electrodynamics do not discuss the corresponding sources. Instead, the source of the FFP electromagnetic field found here can be clearly identified with the Hadronic degrees of freedom described by the NLSM.

3.3.2 Trajectory of charged particles on the FFP

Here we will draw some qualitative plots of the trajectories of charged test particles (like electrons) on the FFP generated by the gauged solitons.

First of all, it follows from Eq. (3.2.5) that the electric and magnetic fields generated by the gauged solitons are

$$\vec{E} = (E_r, E_\theta, 0) \ , \qquad \vec{B} = (B_r, B_\theta, 0) \ , \tag{3.3.4}$$

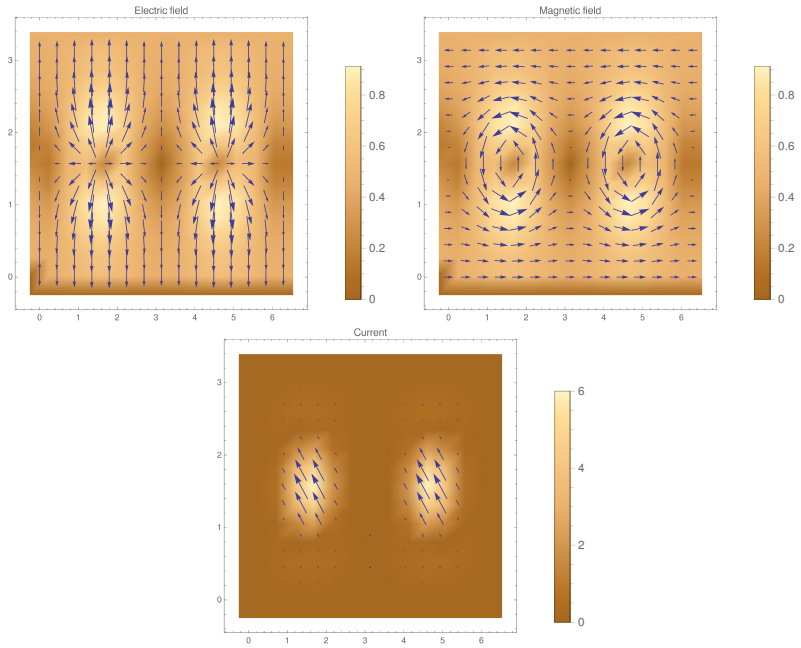

Figure 3.3.1: Electric field, magnetic field and the current of two gauged solitons, with $n = 2$, $m = 0$, and $p = q = 1$. The electric and magnetic fields vanish in the center of the tubes while the current is completely contained inside these.

where the components read

$$E_r = -\partial_r u \ , \quad E_\theta = -\partial_\theta u \ , \quad B_r = \frac{1}{L^3}\partial_\theta u \ , \quad B_\theta = -\frac{1}{L^3}\partial_r u \ . \tag{3.3.5}$$

For a test particle of charge q_e and velocity $\vec{v}$, the Lorentz force generated by the FFP acting on the particle is

$$\vec{F} \ = \ q_e(\vec{E} + \vec{v} \times \vec{B}) \ , \tag{3.3.6}$$

with $\vec{v} = (v_r, v_\theta, v_\phi)$.

Eq. (3.3.6) is a set of three coupled differential equations, namely

$$\frac{m}{q_e}\frac{d^2 r}{dt^2} \ = E_r - B_\theta \frac{d\phi}{dt} \ , \tag{3.3.7}$$

$$\frac{m}{q_e}\frac{d^2 \theta}{dt^2} \ = E_\theta + B_r \frac{d\phi}{dt} \ , \tag{3.3.8}$$

$$\frac{m}{q_e}\frac{d^2 \phi}{dt^2} \ = B_\theta \frac{dr}{dt} - B_r \frac{d\theta}{dt} \ . \tag{3.3.9}$$

The above equations can be numerically integrated to know the trajectory of test

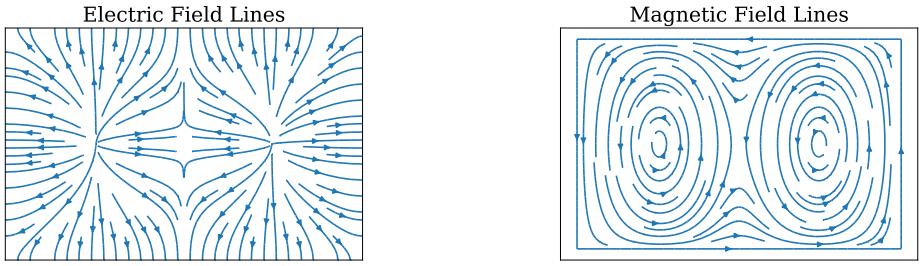

(a) **(b)**

Figure 3.3.2: Electric field lines and magnetic field lines of two gauged solitons, with $n = 2, m = 0$, and $p = q = 1$.

particles. We show the trajectory of a single particle for $0 < t < 1$ in Fig. 3.3.3a, for $1 < t < 50$ in Fig. 3.3.3b and for $490 < t < 500$ in Fig. 3.3.3c.

In these figure one can notice that the charged test particles oscillate in the $r - \theta$ plane while moving along the axis of the tube. It is also worth to emphasize that this motion is quite different from the usual trajectory of a charged test particle in the magnetic field of a thin straight wire. Indeed, in the case of a thin solenoid there is only the $\theta-$component of the magnetic field (and no electric field) while in the present case there is also a radial component and both the electric and the magnetic fields are non-vanishing.

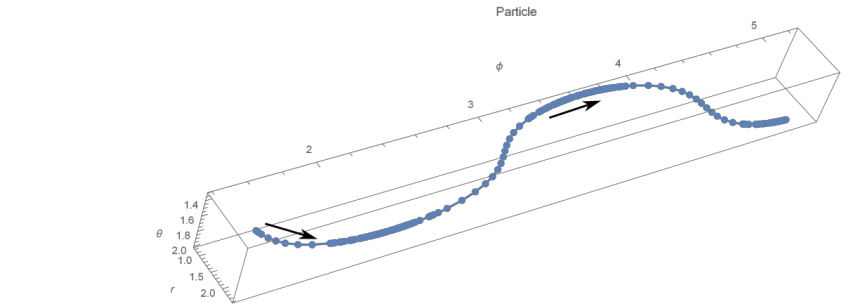

(a)

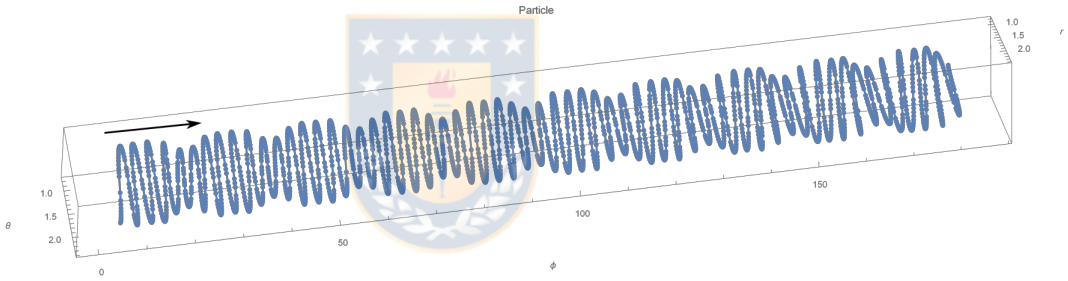

(b)

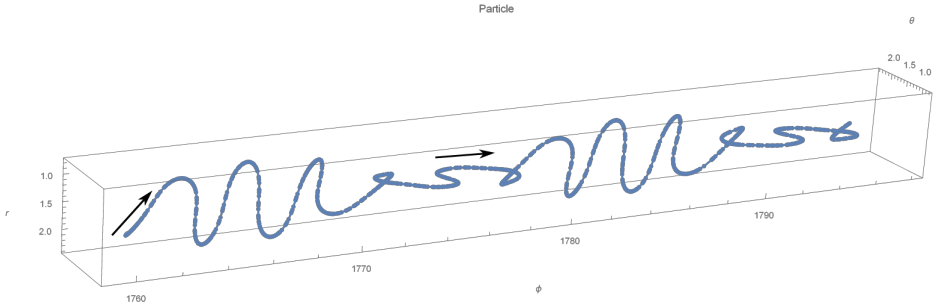

(c)

Figure 3.3.3: Trayectory of a single particle under the Lorentz force in a time interval between 0 and 1 in (a), a time interval between 1 and 50 in (b) and a time interval between 490 and 500 in (c). The arrow denotes the "increasing time direction" on the trajectory of the test particle. The dots on the trajectory have been taken at equal time interval. Thus, regions where neighbouring dots are "far apart" correspond to "high velocity" regions of the trajectory.

Chapter 4

Resurgence in the fluctuations of the fields

In this chapter we perform perturbations of the gauged solitons present in the previous section. From these perturbation emerges Lamé operators which determines the fluctuations of the soliton's background that is to say part of the phonons in the system. This operators are well known from resurgence theory.

On the other hand the electromagnetic perturbations are describes by a two-dimensional Schrodinger equation. We compute numerically the spectrum of this equation and we find that the band are modulated by the strength of the potential.

In the final seccion we show that it is possible to disclose a relation of the present (3+1)-dimensional solitons with the Gross-Neveu model in (1+1)-dimensions (see [83], [81], [73], [74], [82], [9], [10], [11]).

4.1 Pertubative analysis

In this section, we will analyze various perturbations of these gauged solitons. A complete perturbative analysis of these gauged solitons and the corresponding FFP is beyond the scope of the present thesis. First of all, the complete perturbative analysis is a really hard task (not only analytically but also numerically) since it invloves the analysis of seven coupled PDEs in a quite non-trivial background (provided by the gauged solitons and the corresponging FFP themselves). Secondly, it is possible to identify a special class of perturbations of the hadronic field and

of the FFP which has both interesting physical meaning and allows some analytic control.

4.1.1 Perturbations on the U field

A relevant perturbation of these gauged solitons is the one which keeps the hedgehog structure intact. Namely, these are perturbations which keep alive the *hedgehog property* defined in the previous chapter. In the present context such perturbations are defined by the following small deformations of the original ansatz in Eqs. (3.2.2) and (3.2.4):

$$\alpha(r) \to \alpha(r) + \varepsilon f_1(x^\mu) \ , \qquad \Phi(t,\phi) \to \Phi(t,\phi) + \varepsilon f_2(x^\mu) \ , \tag{4.1.1}$$

with $0 < \varepsilon \ll 1$. We will consider

$$f_1(x^\mu) = F_1(r) \ , \qquad f_2(x^\mu) = F_2(r) e^{i(\frac{t}{L} - \phi)} \ . \tag{4.1.2}$$

Such perturbations (and, in particular, the little disturbances f_1 of the profile $\alpha(r)$) are very likely to be the "smallest energy perturbations". The reason is that it takes "a little effort" to perform a radial deformation of α (see, for instance, the discussion of the "hedgehog ansatz" in [75] and [76]) as compared, for instance, to deformations of the Isospin degrees of freedom Θ and Φ. For instance, the classic reference [2] showed that the low energy "Isospin perturbations" have a gap. Hence, there are examples in the literatures in which the unstable negative energy-modes are precisely in this sector while the perturbations of the Isospin degrees of freedom have positive energies. of the hadronic degrees of freedom. For this reason the linear operator which deterimines the spectrum of these perturbations has a very important role.

The field equations in Eq. (3.1.5) at first order in ε for the perturbations defined in Eq. (4.1.1) read

$$\wp_{(1)} F_1 = 0 \ , \qquad \wp_{(2)} F_2 = 0 \ , \tag{4.1.3}$$

where we have defined

$$\wp_{(1)} = -\frac{d^2}{dr^2} + \frac{L_r^2}{KL_\theta^2}\left(Kq^2\cos(2\alpha) - 4L_\theta^2 m^2\cos\alpha\right) \ ,$$
$$\wp_{(2)} = -\frac{d}{dr^2} - \cot(\alpha)\alpha' \ .$$

First of all, one can notice that $F_2(r)$ can be readily integrated giving rise to

$$F_2(r) = \int_1^r c_1 \csc^2(\alpha(\gamma))d\gamma + c_2 \ . \tag{4.1.4}$$

On the other hand the situation for $F_1(r)$ is different. We will write down such linear operator in the case $m = 0$ since in this way the analysis is cleaner, however a non-vanishing m will not change the results and will only make the analytic formulas a bit more involved. In the $m = 0$ case the soliton profile (see Eqs. (3.2.2) and (3.2.7)) is given by

$$\alpha' = \pm\left[2\left(E_0 - \frac{q^2}{4}\frac{L_r^2}{L_\theta^2}\cos(2\alpha)\right)\right]^{\frac{1}{2}} , \quad \alpha(0) = 0 \ , \tag{4.1.5}$$

$$\alpha(r) = \pm\,\mathrm{am}\left(\sqrt{-\frac{L_r^2q^2}{L_\theta^2}}\frac{r}{k}; k\right) \ , \quad k = \sqrt{\frac{2L_r^2q^2}{L_r^2q^2 - 4E_0L_\theta^2}} \ , \tag{4.1.6}$$

where $\mathrm{am}(x;k)$ is the the Jacobi Amplitude ([91], [1]) and k is the elliptic parameter (related to the *elliptic modulus* m in [91], [1] as $k \equiv \sqrt{m}$). From here on we are going to use the parameter k instead m. The periodic structure appears due to the well-known properties of the function $\mathrm{am}(r;k)$, namely

$$\sin\left(\mathrm{am}(r;k)\right) = \mathrm{sn}(r;k) \ , \tag{4.1.7}$$
$$\cos\left(\mathrm{am}(r;k)\right) = \mathrm{cn}(r;k) \ , \tag{4.1.8}$$
$$\sqrt{1 - k^2\sin^2(\mathrm{am}(u,k))} = \mathrm{dn}(u,k) \ , \tag{4.1.9}$$

where $\mathrm{sn}(r;k)$, $\mathrm{cn}(r;k)$ and $\mathrm{dn}(r;k)$ are the Jacobi Elliptic Functions [91].The function $\mathrm{sn}^2(r;k)$ is periodic, with period $2K(k)$, where $K(k) = \int_0^{\pi/2} d\theta/\sqrt{1 - k\sin^2\theta}$ is the elliptic-quarter period.

Going back to the linearized equations, the equation for $F_1(r)$ in Eq. (4.1.3) in

the case $m = 0$ takes the form

$$\wp_{(0)} F_1 = 0 \ , \qquad \wp_{(0)} = -\frac{d^2}{dr^2} + \frac{L_r^2 q^2}{L_\theta^2} \cos(2\alpha) \ . \tag{4.1.10}$$

Quite interestingly, using the properties of Jacobi Amplitudes in Eqs. (4.1.7), (4.1.8) and (4.1.9), the operator $\wp_{(0)}$ (which determines the stability of the present gauged solitons system under the perturbations in Eqs. (4.1.1) and (4.1.2)) can be cast in the form of a Lamé Operator:

$$\wp_{(0)} = -\frac{d^2}{dr^2} + \frac{L_r^2 q^2}{L_\theta^2} (\mathrm{cn}(r/k;k)^2 - \mathrm{sn}(r/k;k)^2) \ . \tag{4.1.11}$$

Consequently, the spectrum of the family of operators $\wp_{(0)}$ (or $\wp_{(m)}$) defined above is very important not only in relation with the stability analysis of the present gauged solitons but also because such spectrum encodes relevant physical informations about the band spectrum of these gauged solitons.

As far as the stability of this gauged solitons-FFP system one need to study the following eigenvalues problem

$$\wp_{(0)} \Psi = \Omega^2 \Psi \ , \tag{4.1.12}$$

so that the stability condition under this family of perturbation is

$$\Omega^2 \geq 0 \ . \tag{4.1.13}$$

It can be seen that the condition in Eq. (4.1.13) can be satisfied. Indeed, it is easy to find a zero mode just taking

$$\Psi_0 = \partial_r \alpha_0 \qquad \Rightarrow \qquad \wp_{(0)} \Psi_0 = 0 \ ,$$

where α_0 is a background solution of Eqs. (4.1.5) and (4.1.6) (or Eq. (3.2.2) in the case with $m \neq 0$). Moreover we can also deduce that Ψ_0 has no node since $\partial_r \alpha_0$ does not vanish. Consequently, standard theorems in Quantum Mechanics ensure that $\Omega^2 = 0$ is the minimal eigenvalue and all the other are positive. In fact, Eq. (4.1.12) encodes many more informations since it has to do with the spectrum of the lowest energy perturbations of the present gauged solitons. In other words, the spectrum of $\wp_{(0)}$ (or $\wp_{(m)}$) will tell us the "phonons" of the system.

In the next section we will analyze such spectrum in the case $m = 0$ in which the results are cleaner and directly related with the theory of resurgence. The results with $m \neq 0$ are very similar but more difficult to analyze with resurgence since such spectrum involves two relevant parameters (this case belongs to the so-called parametric resurgence).

4.1.2 Electromagnetic perturbations

An effective technique to analyze the stability of solutions presented here is to consider the gauged solitons as an effective background medium on which the electromagnetic perturbations propagate. This is an excellent approximation especially in the 't Hooft limit because in the semiclassical Photon-Baryon scattering, the Baryon is basically not affected since the Photon has zero mass (for a detailed discussion see [90]). Consequently, the Photons perceive the gauged soliton as an effective medium while the solitons are not affected by the small fluctuations of the electromagnetic field. Correspondingly, in this section we will consider the $SU(2)$ degrees of freedom as fixed to be the background solution. As it has been already emphasized, the complete stability analysis not only is completely out of reach from analytical methods but also numerically is a very hard task. Nevertheless, the perturbations we are considering here encode relevant features of the gauged solitons and of the corresponding FFP, as we will see below.

Let us consider the following perturbations on the Maxwell potential

$$(u, 0, 0, -Lu) \to (u + \varepsilon\xi_1(x^\mu), 0, 0, -Lu + \varepsilon\xi_2(x^\mu)) \ , \tag{4.1.14}$$

with $0 < \varepsilon \ll 1$. At first order in the parameter ε and for the perturbation defined in Eq. (4.1.14) the Maxwell equations in Eq. (3.1.6) become

$$\begin{aligned}
\partial_\theta(\partial_\phi\xi_2 - L^2\partial_t\xi_1) &= 0 \ , \\
\partial_r(\partial_\phi\xi_2 - L^2\partial_t\xi_1) &= 0 \ , \\
\left(\frac{1}{L_r^2}\partial_r^2 + \frac{1}{L_\theta^2}\partial_\theta^2 + \frac{1}{L^2}\partial_\phi^2\right)\xi_1 - \frac{1}{L^2}\partial_\phi\partial_t\xi_2 + 4K\sin^2(\alpha)\sin^2(q\theta)\xi_1 &= 0 \ , \\
\left(\frac{1}{L_r^2}\partial_r^2 + \frac{1}{L_\theta^2}\partial_\theta^2 - \partial_t^2\right)\xi_2 + \partial_\phi\partial_t\xi_1 + 4K\sin^2(\alpha)\sin^2(q\theta)\xi_2 &= 0 \ .
\end{aligned}$$

Since we want to test linear stability we need to check the (absence of) growing

modes in time. This implies that ξ_1 and ξ_2 must depend on the temporal coordinate. But, according to the previous equations if ξ_1 and ξ_2 depend on time these functions must also depend on the coordinate ϕ, that is

$$\partial_t \xi_i \neq 0 \quad \Rightarrow \partial_\phi \xi_i \neq 0 \ , \qquad \xi_i = \{\xi_1, \xi_2\} \ . \tag{4.1.15}$$

For simplicity we will assume that

$$\partial_\phi \xi_2 = L^2 \partial_t \xi_1, \tag{4.1.16}$$

so that the above equations system is reduced to

$$\Box \xi_i + V \xi_i \ = \ 0 \ , \qquad \Box \equiv -\partial_t^2 + \frac{1}{L_r^2}\partial_r^2 + \frac{1}{L_\theta^2}\partial_\theta^2 + \frac{1}{L^2}\partial_\phi^2 \ ,$$

with $V = 4K \sin^2(\alpha) \sin^2(q\theta)$. Then, performing the Fourier transformation in the coordinate ϕ and time t,

$$\xi_i(t, r, \theta, \phi) \ = \ \int \widehat{\xi_i}(\omega, r, \theta, k_3) e^{-i(k_3\phi + \omega t)} dk_3 d\omega \ ,$$

we obtain an eigenvalue equation for $\hat{\xi}_i$,

$$-\Delta \widehat{\xi_i} + V_{\text{eff}} \widehat{\xi_i} \ = \ \omega^2 \widehat{\xi_i} \ , \tag{4.1.17}$$

with

$$\Delta = \frac{1}{L_r^2}\partial_r^2 + \frac{1}{L_\theta^2}\partial_\theta^2 \ , \qquad V_{\text{eff}} = \frac{(k_3)^2}{L^2} - V \ , \ k_3 \neq 0 \ , \tag{4.1.18}$$

The non-vanishing eigenvalue

$$k_3 = \frac{l}{(2\pi)} \tag{4.1.19}$$

in the effective potential in Eq. (4.1.18) is the wave-number along the ϕ-direction, with l a non-vanishing integer. A sufficient condition ensuring linear stability under the perturbation defined in Eqs. (4.1.15) and (4.1.16) is the requirement

$$V_{\text{eff}} > 0 \ , \tag{4.1.20}$$

where V_{eff} is defined in Eq. (4.1.18). The obvious reason is that the above condition

implies that the eigenvalues E of the operator $\widehat{O}_S$ defined as

$$\widehat{O}_S = -\Delta + V_{\text{eff}}$$

are positive and, consequently, the ω in the time-Fourier transform of the perturbations is real (so that there are no growing modes in time).

However, this condition is not necessary in the sense that it could be possible for V_{eff} to be "slightly negative" keeping, at the same time, the eigenvalue ω^2 in Eq. (4.1.17) real and positive. On the other hand, the mathematical task to find a sharp characterization of the stability in this sector can be very complicated from the viewpoint of functional analysis in the case of Schrodinger-like potentials which depend in a non-trivial way on two (or more) spatial coordinates. Hence, here we will only consider the criterion in Eq. (4.1.20) which is more than enough to provide a qualitative picture. We hope to come back on this interesting mathematical issue in a future publication.

The requirement in Eq. (4.1.20) imposes an upper bound for the length of the box. This can be seen as follows. The "less favorable case" (from the stability viewpoint) corresponds to the least possible value for $(k_3)^2$ in Eq. (4.1.19) when the positive part of the effective potential is the smallest. Correspondingly, Eq. (4.1.20) becomes

$$\frac{(k_3)^2}{L^2} - 4K > 0 \;\Rightarrow \tag{4.1.21}$$

$$L < \frac{1}{4\pi\sqrt{K}} \approx 1 \; fm \; . \tag{4.1.22}$$

In terms of Baryon density, the above bound implies that the present configurations are viable when the Baryon density is of the order of 1 Baryon per fm^3 or higher (this range is well within the range of validity of the NLSM). In fact, we expect that a more refined mathematical analysis would give a better bound showing that these solutions are viable even at lower densities.

4.2 Resurgence Structures in the fluctuations

As it has been described in the previous sections, the perturbations for the $SU(2)$ field are governed by operators with a well-established resurgence character such as the Lamé operator. The singularities analysis (using, for instance, the Borel-Pade

approximation) of these operators in the Borel plane of the effective coupling constant is crucial in order to understand the resurgent character of these type of perturbations. This will be done in the next subsection.

Although resurgence techniques in one-dimensional quantum mechanical system are very well tested, in the case of two-dimensional (and, indeed, higher dimensional) potentials the situation is far less clear. Since the electromagnetic perturbations satisfy an effective two-dimensional Schrodinger equation, the spectrum of the electromagnetic perturbations has been determined numerically. In the following subsections we will describe the numerical results related to the electromagnetic perturbations determined by the two-dimensional Schrödinger (4.2.1) equation

$$-\frac{1}{L_r^2}\frac{\partial^2}{\partial r^2}\Psi(r,\theta)-\frac{1}{L_\theta^2}\frac{\partial^2}{\partial\theta^2}\Psi(r,\theta)+(\frac{k^2}{L^2}-4K\sin^2(\alpha)\sin^2(q\theta))\Psi(r,\theta)=\omega^2\Psi(r,\theta)\ . \tag{4.2.1}$$

4.2.1 WKB Analysis for the SU(2) perturbations

We study a Schrodinger Equation

$$-\frac{g^2}{2}\frac{d^2\psi}{dx^2}+V(x)\psi=u\psi \tag{4.2.2}$$

with the potential

$$V(x)=\mathrm{cn}^2\left(x/k;k\right)-\mathrm{sn}^2\left(x/k;k\right) \tag{4.2.3}$$

This potential is especially well-suited for the resurgence analysis as it has been shown in [41], [8] and [15]. One of the main results of this section is that the proper resurgent parameter g (in the $m=0$ case) is

$$\frac{1}{g^2}=\frac{L_r^2q^2}{L_\theta^2}\ . \tag{4.2.4}$$

Although this result is very simple (one just needs to compare Eq. (4.1.11) with those in [41], [8] and [15]) it is very non-trivial. It is relevant to note that the

effective resurgent parameter[1] g don't involve the coupling constant of the theory, namely K. Instead, the direct computation discussed in this section shows that the suitable parameter is in Eq. (4.2.4), which depends on the odd integer q as well as on the "asymmetry ratio" $\frac{L_r^2}{L_\theta^2}$ which defines how far from a square is the basis in the $r-\theta$ plane of the box in which these gauged solitons are living. The reason why we were able to derive this result explicitly is "just" that we have constructed analytically these gauged solitons which are sources of FFP. Without analytical solutions it would be impossible a proper identification of the correct resurgent parameter.

It is worth to emphasize the similarity of the spectrum of the "phonons" defined by the operator in Eq. (4.1.12) with the ones of the crystal of kinks in [80] as well as in the analysis of the small fluctuations of solitons crystals in integrable field theory models in (1+1) dimensions. In the next section we will elaborate more on this comparison.

We show the Energy spectrum in Fig. 4.2.1 as a function of the coupling g (see Eq. (4.2.4)). We employ the WKB method to obtain an expansion in $g^2 \to 0$. We make an ansatz

$$\Psi(x) = \exp\left(\frac{i}{g^2}\int_{x_0}^{0} dx S(x)\right) \tag{4.2.5}$$

This is an standard procedure in which one solve the resulting Ricatti equation by power series ansatz for $S(x)$ and the Energy

$$S(x) = \sum_{n=0} g^{2n} S_n(x), \quad E = \sum_{n\geq 0} a_n g^{2n} \tag{4.2.6}$$

We use the BenderWu package [79] to compute WKB expansion so that we obtain a perturbative asymptotic expansion of the ground state energy (we will not consider higher level states in this paper).

[1] One of the requirements to be a "good resurgent parameter" is that, for instance, it should determine the spectrum of the small fluctuation of the profile. In particular, when moving the parameter from small to large, one should get the transition in the spectrum from small gaps to large gaps as in the Mathieu equation [41].

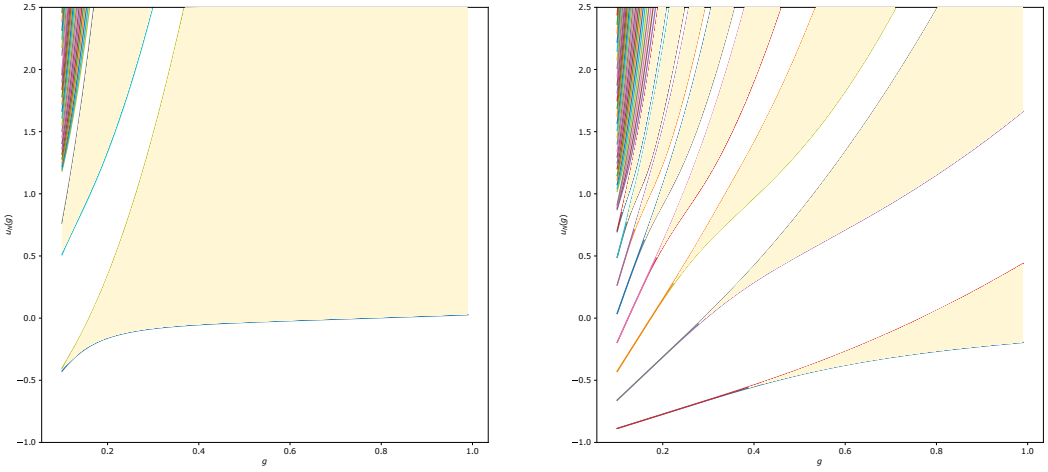

(a) **(b)**

Figure 4.2.1: Energy Spectrum for Lamé operators from $SU(2)$ perturbations for $m = 0.2$ in (a) and $m = 0.7$ in (b). The regions of stability (the bands) are shaded and they are separated by regions of instability (gaps), which are unshaded. We see a similar behaviour to the Mathieu spectrum in wich at small g, the bands are exponentially narrow and high in the spectrum, the gaps are exponentially narrow.

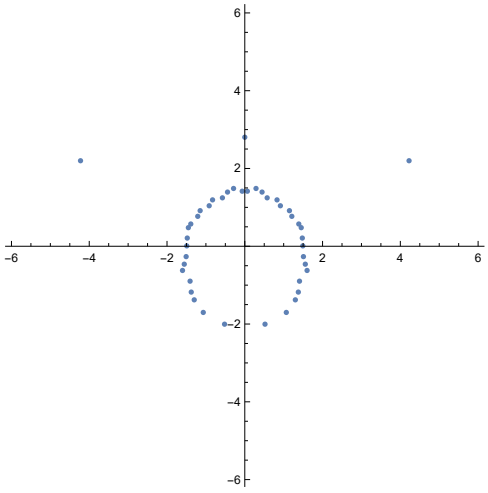

Figure 4.2.2: The complex Borel plane for elliptic modulus $m = 0.9$, dots indicating poles of the Borel-Padé approximation obtained from 100 orders of perturbation theory in g^2 (hence we computed a total of 50 poles). Accumulations of poles are anticipated to encode branch cuts in the full Borel transform, and isolated poles are expected to be residuals of the numerical approximation.

4.2.2 Numerical Results

We present numerical solutions for the two dimensional eigenvalue problem in Eq. (4.2.1) using finite difference method. We considered a two dimensional grid in the (r, θ)-plane of $N_r \times N_\theta$ grid of 70×70 on a domain delimited by $0 < r < 2\pi$ and $0 < \theta < \pi$. We use the Library *Linear algebra* (scipy.linalg) of Python for the eigenvalues problems.

For the numerically implementation we are going to consider the case $L_r = L_\theta = L$. For this case the gauged non-linear sigma model field equations and the perturbed Maxwell equations reads

$$\alpha'' - \frac{q^2}{2}\sin(2\alpha) + \frac{4m^2}{K}\sin(\alpha) = 0 \tag{4.2.7}$$

The boundary for the field α are $\alpha(2\pi) - \alpha(0) = n\pi$. The Topological charge density is directly related with the boundary conditions through the parameter n in the sense it is equal to number of "peaks" of the potential in the r-direction (see Figure 4.2.3).

$$-\left(\frac{\partial^2}{\partial r^2} + \frac{\partial^2}{\partial \theta^2}\right)\Psi + \left(\frac{k^2}{L^2} - 4KL^2\sin^2(\alpha(r))\sin^2(q\theta)\right)\Psi = E\Psi \tag{4.2.8}$$

In this case the potential is fully determined by fixing the parameters q, K and m. In Figure 4.2.4 we plot the energy eigenvalues as a function of L. Making the comparison with the one dimensional Mathieu system [41] (where the band-gaps are modulated by $\hbar$) here L plays the role of an effective $\hbar$

4.3 A comparison with the (1+1)-dimensional crystals in the Gross-Neveu model

The Gross-Neveu model (GN in what follows) is one of the most analyzed quantum field theory in (1+1)-dimensions since it shares many non-trivial properties with interacting quantum field theories in (3+1)-dimensions, such as the appearance of non-trivial condensates at non-perturbative level, asymptotic freedom, Chiral symmetry breaking, dimensional transmutation and so on, but can be analyzed with the tools of the integrable models. Such a model is a theory of N Dirac

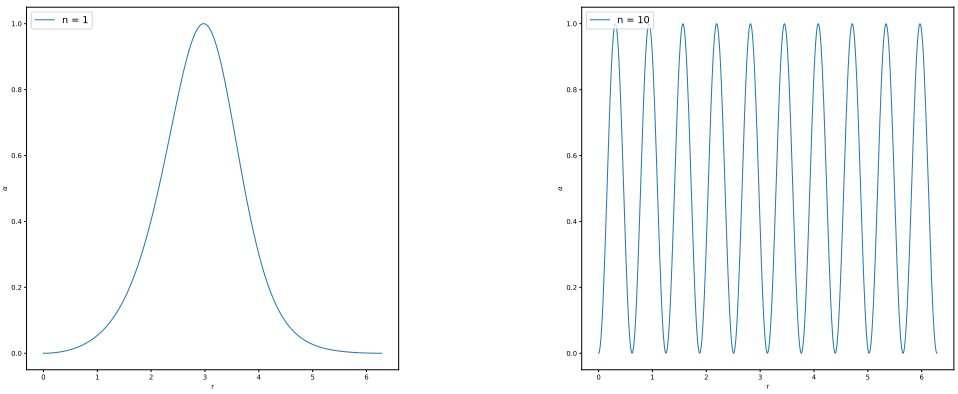

(a) **(b)**

Figure 4.2.3: r-component of two dimensional potential for the perturbed Maxwell equations: $\sin^2(\alpha(r))$ with $n = 1$ and $n = 10$

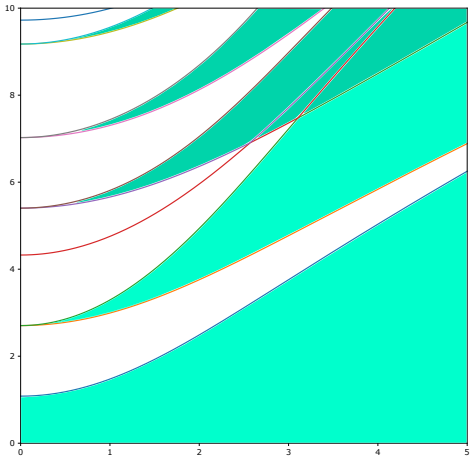

Figure 4.2.4: the Energy Spectrum for the potential $L^2 \sin(\alpha(r))^2 \sin(\theta)^2$ as a function of L, where $\alpha(r)$ is a numerical solution of Eq. (4.2.7) with $n = 1$

fermions interacting via a quartic Fermionic potential, and its Lagrangian is given by

$$\mathcal{L}_{\rm GN} = \sum_{a=1}^{N} \left(i\bar{\psi}_a \gamma^\mu \partial_\mu \psi^a + \frac{g^2}{2} (\bar{\psi}_a \psi^a)^2 \right) \ . \tag{4.3.1}$$

This theory exhibits a phase diagram with a crystalline structure similar to what is expected in QCD, which is invisible to standard perturbation theory being only accessible to the non-perturbative $1/N$ expansion [9], [10], [11]. Using an auxiliary field, the GN field equations can be written as a Hartree-Fock-Dirac equation (see, for instance, [83] and [81]), namely

$$\left(\gamma^5 \frac{1}{i} \frac{\partial}{\partial x} + \gamma^0 S(x) \right) \psi(x) = \omega \psi(x) \ . \tag{4.3.2}$$

The self-consistent analysis of the previous references allows to assume that $S(x)$ is a Lamé potential leading to an analytical solution for the GN model describing a crystal of kinks at finite density. The upper component of the Dirac spinor ϕ_+ corresponds to an Elliptic Function and satisfies a Schrödinger equation

$$\left(-\frac{\partial^2}{\partial \xi^2} + 2\kappa^2 \, \mathrm{sn}^2 \left(\xi | \kappa^2 \right) \right) \phi_+ = \mathcal{E} \phi_+ \ , \tag{4.3.3}$$

where

$$\mathcal{E} = \frac{a^2}{\ell^2} \omega^2 + \kappa^2 \ . \tag{4.3.4}$$

The eigenvalue term $\mathcal{E}$ depends of the constants a, ℓ which are fixed by the mean density. The elliptic parameter κ is fixed by minimized the ground state energy density

$$E_{\rm gs} = -2 \frac{\ell^2}{a^2} \int_{k_{\rm min}}^{k_{\rm max}} \frac{\mathrm{d}k}{2\pi} \sqrt{\mathcal{E} - \kappa^2} + \frac{\ell}{2Ng^2a^2} \int_0^\ell \mathrm{d}\xi \tilde{S}^2(\xi) \equiv E_1 + E_2 \ . \tag{4.3.5}$$

It is relevant to note the close similarity of the results in the references [81], [73], [74], [82], [9], [10], [11] and [80] in the case of the solitons crystals in (1+1)-dimensions with the (3+1)-dimensional gauged solitons discussed here. Not only the energy density of the solitons crystal of the GN model and of the Sine-Gordon model in [80] are very similar to the energy density of the present gauged solitons. This similarity is especially clear comparing the form of the reduced energy density defined in Eqs. (3.2.20) and (3.2.23) with, for instance, the corresponding expression in [80]. Also, the spectrum of the fluctuations of these (1+1)-dimensional solitons crystals

in [81], [73], [74], [82], [9], [10], [11] and [80] are determined by a one-dimensional Schrödinger operator of the same Lamé family as the one in Eq. (4.1.11). This supports very strongly the existence of non-homogeneous condensates in the low energy limit of QCD in (3+1)-dimensions.

Chapter 5

Conclusions

In this thesis we have shown analytically that topologically non-trivial gauged solitons of the (3+1)-dimensional gauged non-linear sigma model at finite Baryon density are natural sources of Force Free Plasma. For these multi-solitons most of the total energy and the topological charge are gathered within tube-shaped regions while the magnetic field lines go around the tubes. Our explicit analytical solutions allow to discuss the trajectories of charged test particles moving close to these gauged solitons and also identify the proper resurgent parameters through the analysis of the perturbations. In particular, the perturbations of the solitons profile are related to Lamé operators with a suitable resurgent parameter. On the other hand, the electromagnetic perturbations of the above system satisfy a two dimensional effective Schrödinger equation, where the soliton's background interacts with the electromagnetic perturbations through an effective periodic potential in two spatial dimensions. Also we studied numerically the band energy spectrum for different values of the free parameters of the theory and we found that bands-gaps are modulated by the potential strength. Finally we have shown that the crystal solutions constructed here are qualitatively very similar to those of the Gross-Neveu model in (1+1) dimensions, which strongly support the existence of non-homogeneous condensates in the low energy limit of QCD in (3+1)-dimensions.

At a last remark it is worth to say that all the analysis both resurgence and physical aspects of these gauged solitons is possible because we have analytical solutions of the NLSM coupled to Maxwell. Otherwise it would have been impossible to shed light on ideas as abstract as those of resurgence even in (3+1)-dimensions.

Bibliography

[1] M. Abramowitz. *Handbook of Mathematical Functions, With Formulas, Graphs, and Mathematical Tables,*. Dover Publications, Inc., USA, 1974. ISBN 0486612724.

[2] G. S. Adkins, C. R. Nappi, and E. Witten. Static Properties of Nucleons in the Skyrme Model. *Nucl. Phys. B*, 228:552, 1983. doi: 10.1016/0550-3213(83)90559-X.

[3] P. D. Alvarez, S. L. Cacciatori, F. Canfora, and B. L. Cerchiai. Analytic SU(N) Skyrmions at finite Baryon density. *Phys. Rev. D*, 101(12):125011, 2020. doi: 10.1103/PhysRevD.101.125011.

[4] I. Aniceto and R. Schiappa. Nonperturbative Ambiguities and the Reality of Resurgent Transseries. *Commun. Math. Phys.*, 335(1):183–245, 2015. doi: 10.1007/s00220-014-2165-z.

[5] I. Aniceto, J. G. Russo, and R. Schiappa. Resurgent Analysis of Localizable Observables in Supersymmetric Gauge Theories. *JHEP*, 03:172, 2015. doi: 10.1007/JHEP03(2015)172.

[6] I. Aniceto, G. Başar, and R. Schiappa. A primer on resurgent transseries and their asymptotics. *Physics Reports*, 809:1–135, 2019.

[7] G. Başar and G. V. Dunne. Resurgence and the Nekrasov-Shatashvili limit: connecting weak and strong coupling in the Mathieu and Lamé systems. *JHEP*, 02:160, 2015. doi: 10.1007/JHEP02(2015)160.

[8] G. Başar and G. V. Dunne. Resurgence and the Nekrasov-Shatashvili limit: connecting weak and strong coupling in the Mathieu and Lamé systems. *JHEP*, 02:160, 2015. doi: 10.1007/JHEP02(2015)160.

[9] G. m. c. Başar and G. V. Dunne. Self-consistent crystalline condensate in chiral gross-neveu and bogoliubov–de gennes systems. *Phys. Rev. Lett.*, 100:200404, May 2008. doi: 10.1103/PhysRevLett.100.200404. URL https://link.aps.org/doi/10.1103/PhysRevLett.100.200404.

[10] G. m. c. Başar and G. V. Dunne. Twisted kink crystal in the chiral gross-neveu model. *Phys. Rev. D*, 78:065022, Sep 2008. doi: 10.1103/PhysRevD.78.065022. URL https://link.aps.org/doi/10.1103/PhysRevD.78.065022.

[11] G. m. c. Başar, G. V. Dunne, and M. Thies. Inhomogeneous condensates in the thermodynamics of the chiral njl_2 model. *Phys. Rev. D*, 79:105012, May 2009. doi: 10.1103/PhysRevD.79.105012. URL https://link.aps.org/doi/10.1103/PhysRevD.79.105012.

[12] A. P. Balachandran, A. Barducci, F. Lizzi, V. G. J. Rodgers, and A. Stern. Doubly strange dibaryon in the chiral model. *Phys. Rev. Lett.*, 52:887–890, Mar 1984. doi: 10.1103/PhysRevLett.52.887. URL https://link.aps.org/doi/10.1103/PhysRevLett.52.887.

[13] A. P. Balachandran, G. Marmo, B. S. Skagerstam, and A. Stern. *Classical Topology and Quantum States*. WORLD SCIENTIFIC, 1991. doi: 10.1142/1180. URL https://www.worldscientific.com/doi/abs/10.1142/1180.

[14] Balachandran, A. P. and Nair, V. P. and Panchapakesan, N and Rajeev, S.G. Low-mass solitons from fractional charges in quantum chromodynamics. *Rev. Phys. D*, 28:2830, 1983.

[15] G. Basar, G. V. Dunne, and M. Unsal. Resurgence theory, ghost-instantons, and analytic continuation of path integrals. *JHEP*, 10:041, 2013. doi: 10.1007/JHEP10(2013)041.

[16] G. L. Bayatian et al. CMS technical design report, volume II: Physics performance. *J. Phys. G*, 34(6):995–1579, 2007. doi: 10.1088/0954-3899/34/6/S01.

[17] C. M. Bender and T. T. Wu. Anharmonic oscillator. 2: A Study of perturbation theory in large order. *Phys. Rev. D*, 7:1620–1636, 1973. doi: 10.1103/PhysRevD.7.1620.

[18] D. K. Berry, M. E. Caplan, C. J. Horowitz, G. Huber, and A. S. Schneider. "Parking-garage" structures in nuclear astrophysics and cellular biophysics. *Phys. Rev. C*, 94(5):055801, 2016. doi: 10.1103/PhysRevC.94.055801.

[19] R. D. Blandford and R. L. Znajek. Electromagnetic extractions of energy from Kerr black holes. *Mon. Not. Roy. Astron. Soc.*, 179:433–456, 1977. doi: 10.1093/mnras/179.3.433.

[20] E. B. Bogomolny. CALCULATION OF INSTANTON - ANTI-INSTANTON CONTRIBUTIONS IN QUANTUM MECHANICS. *Phys. Lett. B*, 91:431–435, 1980. doi: 10.1016/0370-2693(80)91014-X.

[21] N. Brambilla et al. QCD and Strongly Coupled Gauge Theories: Challenges and Perspectives. *Eur. Phys. J. C*, 74(10):2981, 2014. doi: 10.1140/epjc/s10052-014-2981-5.

[22] T. D. Brennan and S. E. Gralla. On the magnetosphere of an accelerated pulsar. *Phys. Rev. D*, 89:103013, May 2014. doi: 10.1103/PhysRevD.89.103013. URL https://link.aps.org/doi/10.1103/PhysRevD.89.103013.

[23] T. D. Brennan, S. E. Gralla, and T. Jacobson. Exact solutions to force-free electrodynamics in black hole backgrounds. *Classical and Quantum Gravity*, 30(19):195012, sep 2013. doi: 10.1088/0264-9381/30/19/195012. URL https://doi.org/10.1088/0264-9381/30/19/195012.

[24] C. G. Callan, Jr. and E. Witten. Monopole Catalysis of Skyrmion Decay. *Nucl. Phys. B*, 239:161–176, 1984. doi: 10.1016/0550-3213(84)90088-9.

[25] F. Canfora. Ordered arrays of Baryonic tubes in the Skyrme model in ($3+1$) dimensions at finite density. *Eur. Phys. J. C*, 78(11):929, 2018. doi: 10.1140/epjc/s10052-018-6404-x.

[26] F. Canfora, S. H. Oh, and A. Vera. Analytic crystals of solitons in the four dimensional gauged non-linear sigma model. *Eur. Phys. J. C*, 79(6):485, 2019. doi: 10.1140/epjc/s10052-019-6994-y.

[27] F. Canfora, M. Lagos, and A. Vera. Crystals of superconducting Baryonic tubes in the low energy limit of QCD at finite density. *Eur. Phys. J. C*, 80 (8):697, 2020. doi: 10.1140/epjc/s10052-020-8275-1.

[28] M. E. Caplan, A. S. Schneider, and C. J. Horowitz. Elasticity of Nuclear Pasta. *Phys. Rev. Lett.*, 121(13):132701, 2018. doi: 10.1103/PhysRevLett.121.132701.

[29] K. G. Chetyrkin, J. H. Kuhn, and C. Sturm. Four-loop moments of the heavy quark vacuum polarization function in perturbative QCD. *Eur. Phys. J. C*, 48:107–110, 2006. doi: 10.1140/epjc/s2006-02610-y.

[30] G. Compère and R. Oliveri. Near-horizon extreme kerr magnetospheres. *Phys. Rev. D*, 93:024035, Jan 2016. doi: 10.1103/PhysRevD.93.024035. URL https://link.aps.org/doi/10.1103/PhysRevD.93.024035.

[31] O. Costin. *Asymptotics and Borel Summability*. Chapman Hall/CRC, 2009.

[32] P. de Forcrand. Simulating QCD at finite density. *PoS*, LAT2009:010, 2009. doi: 10.22323/1.091.0010.

[33] E. Delabae. *Introduction to the Ecalle theory*. Cambridge University Pres, 1994.

[34] S. Demulder, D. Dorigoni, and D. C. Thompson. Resurgence in η-deformed Principal Chiral Models. *JHEP*, 07:088, 2016. doi: 10.1007/JHEP07(2016)088.

[35] G. H. Derrick. Comments on nonlinear wave equations as models for elementary particles. *J. Math. Phys.*, 5:1252–1254, 1964. doi: 10.1063/1.1704233.

[36] D. Dorigoni. An introduction to resurgence, trans-series and alien calculus. *Annals of Physics*, 409, 2019.

[37] G. V. Dunne and M. Unsal. Resurgence and Trans-series in Quantum Field Theory: The CP(N-1) Model. *JHEP*, 11:170, 2012. doi: 10.1007/JHEP11(2012)170.

[38] G. V. Dunne and M. Ünsal. Continuity and Resurgence: towards a continuum definition of the $\mathbb{CP}$(N-1) model. *Phys. Rev. D*, 87:025015, 2013. doi: 10.1103/PhysRevD.87.025015.

[39] G. V. Dunne and M. Ünsal. Generating nonperturbative physics from perturbation theory. *Phys. Rev. D*, 89(4):041701, 2014. doi: 10.1103/PhysRevD.89.041701.

[40] G. V. Dunne and M. Unsal. Uniform WKB, Multi-instantons, and Resurgent Trans-Series. *Phys. Rev. D*, 89(10):105009, 2014. doi: 10.1103/PhysRevD.89.105009.

[41] G. V. Dunne and M. Ünsal. Wkb and resurgence in the mathieu equation. In F. Fauvet, D. Manchon, S. Marmi, and D. Sauzin, editors, *Resurgence, Physics and Numbers*, pages 249–298, Pisa, 2017. Scuola Normale Superiore. ISBN 978-88-7642-613-1.

[42] G. V. Dunne, M. Shifman, and M. Unsal. Infrared Renormalons versus Operator Product Expansions in Supersymmetric and Related Gauge Theories. *Phys. Rev. Lett.*, 114(19):191601, 2015. doi: 10.1103/PhysRevLett.114.191601.

[43] F. J. Dyson. Divergence of perturbation theory in quantum electrodynamics. *Phys. Rev.*, 85:631–632, Feb 1952. doi: 10.1103/PhysRev.85.631. URL https://link.aps.org/doi/10.1103/PhysRev.85.631.

[44] J. Écalle. Les fonctions resurgentes. *Publ. Math. Orsay*, I-III, 1981.

[45] J. Gasser and H. Leutwyler. Chiral Perturbation Theory: Expansions in the Mass of the Strange Quark. *Nucl. Phys. B*, 250:465–516, 1985. doi: 10.1016/0550-3213(85)90492-4.

[46] T. Gold. Rotating neutron stars as the origin of the pulsating radio sources. *Nature*, 218:731–732, 1968. doi: 10.1038/218731a0.

[47] P. Goldreich and W. H. Julian. Pulsar Electrodynamics. *apj*, 157:869, Aug. 1969. doi: 10.1086/150119.

[48] S. E. Gralla and T. Jacobson. Spacetime approach to force-free magnetospheres. *Monthly Notices of the Royal Astronomical Society*, 445(3):2500–2534, 10 2014. ISSN 0035-8711. doi: 10.1093/mnras/stu1690. URL https://doi.org/10.1093/mnras/stu1690.

[49] S. E. Gralla and T. Jacobson. Nonaxisymmetric poynting jets. *Phys. Rev. D*, 92:043002, Aug 2015. doi: 10.1103/PhysRevD.92.043002. URL https://link.aps.org/doi/10.1103/PhysRevD.92.043002.

[50] S. E. Gralla, A. Lupsasca, and M. J. Rodriguez. Electromagnetic jets from stars and black holes. *Phys. Rev. D*, 93:044038, Feb 2016. doi: 10.1103/PhysRevD.93.044038. URL https://link.aps.org/doi/10.1103/PhysRevD.93.044038.

[51] J. Greensite. *An introduction to the confinement problem*, volume 821. Springer-Verlag Berlin Heidelberg, 2011. doi: 10.1007/978-3-642-14382-3.

[52] Hashimoto, M. and Seki, H. and Yamada, M. Shape of nuclei in the crust of a neutron star. *Prog. Theor. Phys.*, 71:320, 1984.

[53] C. J. Horowitz, D. K. Berry, C. M. Briggs, M. E. Caplan, A. Cumming, and A. S. Schneider. Disordered nuclear pasta, magnetic field decay, and crust cooling in neutron stars. *Phys. Rev. Lett.*, 114(3):031102, 2015. doi: 10.1103/PhysRevLett.114.031102.

[54] Kobyakov, D.N. and Pethick, C.J. Superfluid Liquid Crystals: Pasta Phases in Neutron Star Crusts. *J. Exp. Theor. Phys.*, 127:851–859, 2018.

[55] J.-P. Lasota, E. Gourgoulhon, M. Abramowicz, A. Tchekhovskoy, and R. Narayan. Extracting black-hole rotational energy: The generalized penrose process. *Phys. Rev. D*, 89:024041, Jan 2014. doi: 10.1103/PhysRevD.89.024041. URL https://link.aps.org/doi/10.1103/PhysRevD.89.024041.

[56] L. N. Lipatov. Divergence of the Perturbation Theory Series and the Quasiclassical Theory. *Sov. Phys. JETP*, 45:216–223, 1977.

[57] A. Lupsasca and M. J. Rodriguez. Exact Solutions for Extreme Black Hole Magnetospheres. *JHEP*, 07:090, 2015. doi: 10.1007/JHEP07(2015)090.

[58] A. Lupsasca, M. J. Rodriguez, and A. Strominger. Force-Free Electrodynamics around Extreme Kerr Black Holes. *JHEP*, 12:185, 2014. doi: 10.1007/JHEP12(2014)185.

[59] D. MacDonald and K. S. Thorne. Black-hole electrodynamics - an absolute-space/universal-time formulation. *Mon. Not. Roy. Astron. Soc.*, 198:345–383, 1982.

[60] N. Manton and P. Sutcliffe. *Topological Solitons*. Cambridge Monographs on Mathematical Physics. Cambridge University Press, 2004. doi: 10.1017/CBO9780511617034.

[61] N. Manton and P. Sutcliffe. *Topological Solitons*. Cambridge University Press, Cambridge, 2007.

[62] M. Mariño and T. Reis. Resurgence for superconductors. *J. Stat. Mech.*, 5 2019. doi: 10.1088/1742-5468/ab4802.

[63] M. Marino, R. Schiappa, and M. Weiss. Nonperturbative Effects and the Large-Order Behavior of Matrix Models and Topological Strings. *Commun. Num. Theor. Phys.*, 2:349–419, 2008. doi: 10.4310/CNTP.2008.v2.n2.a3.

[64] M. Mariño. Lectures on non-perturbative effects in large n gauge theories, matrix models and strings. *Fortschritte der Physik*, 62(5-6):455–540, 2014. doi: https://doi.org/10.1002/prop.201400005. URL https://onlinelibrary.wiley.com/doi/abs/10.1002/prop.201400005.

[65] M. Mariño. Lectures on non-perturbative effects in large n gauge theories, matrix models and strings. *Fortschritte der Physik*, 62(5-6):455–540, 2014. doi: https://doi.org/10.1002/prop.201400005.

[66] M. Mariño. *Instantons and Large N: An Introduction to Non-Perturbative Methods in Quantum Field Theory*. Cambridge University Press, 2015.

[67] M. Mariño, R. Schiappa, and M. Weiss. Multi-instantons and multicuts. *Journal of Mathematical Physics*, 50(5):052301, 2009. doi: 10.1063/1.3097755.

[68] V. P. Nair. *Quantum Field Theory: A Modern Perspective*. Springer-Verlag New York, 2005. doi: 10.1007/b106781.

[69] F. PACINI. Rotating Neutron Stars, Pulsars and Supernova Remnants. *Nature*, 219:145–146, 1968. doi: 10.1038/219145a0.

[70] B. M. A. G. Piette and D. H. Tchrakian. Static solutions in the U(1) gauged Skyrme model. *Phys. Rev. D*, 62:025020, 2000. doi: 10.1103/PhysRevD.62.025020.

[71] D. Sauzin. Resurgent functions and splitting problem. *RIMS Kokyurok*, 2005.

[72] L. Schepers and D. C. Thompson. Resurgence in the bi-Yang-Baxter model. *Nucl. Phys. B*, 964:115308, 2021. doi: 10.1016/j.nuclphysb.2021.115308.

[73] O. Schnetz, M. Thies, and K. Urlichs. Phase diagram of the gross–neveu model: exact results and condensed matter precursors. *Annals of Physics*, 314(2):425–447, 2004. ISSN 0003-4916. doi: https://doi.org/10.1016/j.aop.2004.06.009. URL https://www.sciencedirect.com/science/article/pii/S0003491604001241.

[74] O. Schnetz, M. Thies, and K. Urlichs. Full phase diagram of the massive gross–neveu model. *Annals of Physics*, 321(11):2604–2637, 2006. ISSN 0003-4916. doi: https://doi.org/10.1016/j.aop.2005.12.007. URL https://www.sciencedirect.com/science/article/pii/S0003491605002915.

[75] M. Shifman. *Advanced Topics in Quantum Field Theory: A Lecture Course*. Cambridge University Press, 2012.

[76] M. Shifman and A. Yung. *Supersymmetric Solitons*. Cambridge University Press, 2009.

[77] T. H. R. Skyrme. A Nonlinear field theory. *Proc. Roy. Soc. Lond. A*, 260:127–138, 1961. doi: 10.1098/rspa.1961.0018.

[78] N. Sueishi, S. Kamata, T. Misumi, and M. Ünsal. On exact-WKB analysis, resurgent structure, and quantization conditions. *JHEP*, 12:114, 2020. doi: 10.1007/JHEP12(2020)114.

[79] T. Sulejmanpasic and M. Ünsal. Aspects of perturbation theory in quantum mechanics: The BenderWuMATHEMATICA package. *Computer Physics Communications*, 228:273–289, July 2018. doi: 10.1016/j.cpc.2017.11.018.

[80] K. Takayama and M. Oka. Bosonic excitations in a crystal of sine-gordon kinks. *Nuclear Physics A*, 551(4):637–656, 1993. ISSN 0375-9474. doi: https://doi.org/10.1016/0375-9474(93)90270-8. URL https://www.sciencedirect.com/science/article/pii/0375947493902708.

[81] M. Thies. Analytical solution of the gross-neveu model at finite density. *Phys. Rev. D*, 69:067703, Mar 2004. doi: 10.1103/PhysRevD.69.067703. URL https://link.aps.org/doi/10.1103/PhysRevD.69.067703.

[82] M. Thies. From relativistic quantum fields to condensed matter and back again: Updating the Gross-Neveu phase diagram. *J. Phys. A*, 39:12707–12734, 2006. doi: 10.1088/0305-4470/39/41/S04.

[83] M. Thies and K. Urlichs. Revised phase diagram of the gross-neveu model. *Phys. Rev. D*, 67:125015, Jun 2003. doi: 10.1103/PhysRevD.67.125015. URL https://link.aps.org/doi/10.1103/PhysRevD.67.125015.

[84] T. Uchida. Theory of force-free electromagnetic fields. i. general theory. *Phys. Rev. E*, 56:2181–2197, Aug 1997. doi: 10.1103/PhysRevE.56.2181. URL https://link.aps.org/doi/10.1103/PhysRevE.56.2181.

[85] T. Uchida. Theory of force-free electromagnetic fields. ii. configuration with symmetry. *Phys. Rev. E*, 56:2198–2212, Aug 1997. doi: 10.1103/PhysRevE.56.2198. URL https://link.aps.org/doi/10.1103/PhysRevE.56.2198.

[86] T. Uchida. Linear perturbations in force-free black hole magnetospheres — I. General theory. *Monthly Notices of the Royal Astronomical Society*, 286 (4):931–947, 04 1997. ISSN 0035-8711. doi: 10.1093/mnras/286.4.931. URL https://doi.org/10.1093/mnras/286.4.931.

[87] T. Uchida. Linear perturbations in force-free black hole magnetospheres — II. Wave propagation. *Monthly Notices of the Royal Astronomical Society*, 291(1):125–144, 10 1997. ISSN 0035-8711. doi: 10.1093/mnras/291.1.125. URL https://doi.org/10.1093/mnras/291.1.125.

[88] T. Uchida. The force-free magnetosphere around an oblique rotator. *Monthly Notices of the Royal Astronomical Society*, 297(1):315–322, 06 1998. ISSN 0035-8711. doi: 10.1046/j.1365-8711.1998.01528.x. URL https://doi.org/10.1046/j.1365-8711.1998.01528.x.

[89] A. I. Vainshtein. Decaying systems and divergence of the series of perturbation theory. In *Continuous Advances in QCD 2002 /*

ARKADYFEST (honoring the 60th birthday of Prof. Arkady Vainshtein), 12 1964.

[90] H. Weigel. *Chiral Soliton Models for Baryons*. Springer-Verlag Berlin Heidelberg, 2008. doi: 10.1007/978-3-540-75436-7.

[91] E. Whittaker and G. Watson. *A Course of ModernAnalysis*. Cambridge University Press, 1927.

[92] T. Wiegelmann and T. Sakurai. Solar force-free magnetic fields. *JOURNAL OF GEOPHYSICAL RESEARCH*, 113, 2012.

[93] T. Wiegelmann and T. Sakurai. Solar force-free magnetic fields. *Living Rev Sol Phys*, 18(1), 2021. URL https://doi.org/10.1007/s41116-020-00027-4.

[94] E. Witten. Global Aspects of Current Algebra. *Nucl. Phys. B*, 223:422–432, 1983. doi: 10.1016/0550-3213(83)90063-9.

[95] H. Yang and F. Zhang. Stability of force-free magnetospheres. *Phys. Rev. D*, 90:104022, Nov 2014. doi: 10.1103/PhysRevD.90.104022. URL https://link.aps.org/doi/10.1103/PhysRevD.90.104022.

[96] F. Zhang, H. Yang, and L. Lehner. Towards an understanding of the force-free magnetosphere of rapidly spinning black holes. *Phys. Rev. D*, 90:124009, Dec 2014. doi: 10.1103/PhysRevD.90.124009. URL https://link.aps.org/doi/10.1103/PhysRevD.90.124009.

[97] F. Zhang, S. T. McWilliams, and H. P. Pfeiffer. Stability of exact force-free electrodynamic solutions and scattering from spacetime curvature. *Phys. Rev. D*, 92:024049, Jul 2015. doi: 10.1103/PhysRevD.92.024049. URL https://link.aps.org/doi/10.1103/PhysRevD.92.024049.

[98] J. Zinn-Justin. Multi - Instanton Contributions in Quantum Mechanics. *Nucl. Phys. B*, 192:125–140, 1981. doi: 10.1016/0550-3213(81)90197-8.

[99] J. Zinn-Justin. Multi-instanton contributions in quantum mechanics. *Nuclear Physics B*, 192(1):125–140, 1981. ISSN 0550-3213. doi: https://doi.org/10.1016/0550-3213(81)90197-8. URL https://www.sciencedirect.com/science/article/pii/0550321381901978.

[100] J. Zinn-Justin and G. J. Le. *Large-order behaviour of perturbation theory*. North Holland, Amsterdam, 1990.

A1 Obtaining the field equations

Explicitly, the $SU(2)$ scalar field, according to our ansatz defined in chapter III is given by

$$U = \begin{pmatrix} \cos(\alpha) + i\cos(q\theta)\sin(\alpha) & ie^{-\frac{ip}{L}(t-L\phi)}\sin(q\theta)\sin(\alpha) \\ ie^{\frac{ip}{L}(t-L\phi)}\sin(q\theta)\sin(\alpha) & \cos(\alpha) - i\cos(q\theta)\sin(\alpha) \end{pmatrix} .$$

It follows that the components of $L_\mu = U^{-1}D_\mu U$ read

$$L_t = \frac{P}{L}\begin{pmatrix} i\sin^2(q\theta)\sin^2(\alpha) & E^{(+)}F^{(-)} \\ -E^{(-)}F^{(+)} & -i\sin^2(q\theta)\sin^2(\alpha) \end{pmatrix} , \quad L_r = i\alpha'\begin{pmatrix} \cos(q\theta) & E^{(+)}\sin(q\theta) \\ E^{(-)}\sin(q\theta) & -\cos(q\theta) \end{pmatrix} ,$$

$$L_\theta = q\sin(\alpha)\begin{pmatrix} -i\sin(q\theta)\cos(\alpha) & E^{(+)}G^{(+)} \\ E^{(-)}G^{(-)} & i\sin(q\theta)\cos(\alpha) \end{pmatrix} , \quad L_\phi = P\begin{pmatrix} -i\sin^2(q\theta)\sin^2(\alpha) & -E^{(+)} \\ E^{(-)}F^{(+)} & i\sin^2(q\theta) \end{pmatrix}$$

where we have defined

$$P = p - 2Lu , \qquad F^{(\pm)} = \Big(\cot(\alpha) \pm i\cos(q\theta)\Big)\sin(q\theta)\sin^2(\alpha) ,$$
$$E^{(\pm)} = e^{\pm i\frac{p}{L}(L\phi - t)} , \qquad G^{(\pm)} = i\cos(q\theta)\cos(\alpha) \pm \sin(\alpha) .$$

On the other hand, varying the Lagrangian w.r.t the U field we obtain

$$\begin{aligned} \delta\mathcal{L} &= \mathrm{Tr}\left[\frac{K}{4}\delta(L^\mu L_\mu) - m^2\delta(U + U^{-1})\right] \\ &= \mathrm{Tr}\left[\frac{K}{2}L^\mu\delta L_\mu - m^2(\delta U + \delta U^{-1})\right] . \end{aligned}$$

For the non-linear sigma model term, we use

$$\begin{aligned} \delta(UU^{-1}) = 0 \quad &\rightarrow \quad \delta U^{-1} = -U^{-1}\delta U U^{-1} , \\ D_\mu(UU^{-1}) = 0 \quad &\rightarrow \quad D_\mu U^{-1} = -U^{-1}D_\mu U U^{-1} = -L_\mu U^{-1} , \end{aligned}$$

so that

$$\begin{aligned}\delta L_\mu &= \delta(U^{-1}D_\mu U)\\ &= -U^{-1}\delta U U^{-1}D_\mu U + U^{-1}\delta D_\mu U\\ &= -U^{-1}\delta U L_\mu + L_\mu U^{-1}\delta U + D_\mu(U^{-1}\delta U)\ . \end{aligned} \tag{A1.1}$$

From the above, the variation of the non-linear sigma model term (using the cyclicity of the trace for the first two terms) becomes

$$\begin{aligned}\mathrm{Tr}(L^\mu \delta L_\mu) &= \mathrm{Tr}(L^\mu D_\mu(U^{-1}\delta U))\\ &= -\mathrm{Tr}(D_\mu L^\mu U^{-1}\delta U) + \mathrm{Tr}(D_\mu(U^{-1}\delta U L^\mu))\ , \end{aligned} \tag{A1.2}$$

where we have integrated by parts. Now, introducing this in the variation of the Lagrangian, we obtain

$$\begin{aligned}\delta\mathcal{L} &= \mathrm{Tr}\left[-\frac{K}{2}D_\mu L^\mu U^{-1}\delta U - m^2(\delta U - U^{-1}\delta U U^{-1})\right] \quad + \quad \text{Boundary term}\\ &= -\mathrm{Tr}\left[\frac{K}{2}D_\mu L^\mu U^{-1}\delta U + m^2(U U^{-1}\delta U - U^{-1}U^{-1}\delta U)\right] \quad + \quad \text{Boundary term}\\ &= -\mathrm{Tr}\left[\left(\frac{K}{2}D_\mu L^\mu + m^2(U - U^{-1})\right)U^{-1}\delta U\right] \quad + \quad \text{Boundary term}\ , \end{aligned}$$

and because $U \neq 0$ and the first factor in the trace is in the algebra, it is necessarily that

$$D_\mu L^\mu + \frac{2m^2}{K}\left(U - U^{-1}\right) = 0\ .$$

Replacing the L_μ in the previous equation we obtain the equation for the soliton profile.